11-29-2016 12:00 AM

Improved Localization Algorithms in Indoor Wireless Environment

Fei Long, *The University of Western Ontario*

Supervisor: Dr. Xianbin Wang, *The University of Western Ontario*
Joint Supervisor: Dr. Jagath Samarabandu, *The University of Western Ontario*
A thesis submitted in partial fulfillment of the requirements for the Master of Engineering Science degree in Electrical and Computer Engineering

Abstract

Localization has been considered as an important precondition for the location-dependent applications such as mobile tracking and navigation.To obtain specific location information, we usually make use of Global Positioning System(GPS), which is the most common platform to acquire localization information in outdoor environments. When targets are in indoor environment, however, the GPS signal is usually blocked, so we also consider other assisted positioning techniques in order to obtain accurate position of targets. In this thesis, three different schemes in indoor environment are proposed to minimize localization error by placing reference nodes in optimum locations, combining the localization information from accelerometer sensor in smartphone with Received Signal Strength (RSS) from reference nodes, and utilizing frequency diversity in Wireless Fidelity (WiFi) environment.

Deployments of reference nodes are vital for locating nearby targets since they are used to estimate the distances from them to the targets. A reference nodes' placement scheme based on minimizing the average mean square error of localization over a certain region is proposed in this thesis first and is applied in different localization regions which are circular, square and hexagonal for illustration of the flexibility of the proposed scheme.

Equipped with accelerometer sensor, smartphone provides useful information which outputs accelerations in three different directions. Combining acceleration information from smartphones and signal strength information from reference nodes to prevent the accumulated error from accelerometer is studied in this thesis. The combined locating error is narrowed by assigning different weights to localization information from accelerometer and reference nodes.

In indoor environment, RSS technology based localization is the most common way to imply since it require less additional hardware compared to other localization technologies. However, RSS can be affected greatly by complex circumstance as well as carrier frequency. Utilization of diverse frequencies to improve localization performance is proposed in the end of this thesis along with some experiments applied on Software Defined Platform (SDR).

Keywords: indoor localization, reference node, accelerometer sensor, Software Defined Radio

Acknowledgements

I would like to express my special appreciation and sincere thanks to my supervisor Professor Dr. Xianbin Wang, you have been a tremendous mentor for me. I would like thank you for encouraging my research and for guiding me to complete this thesis. Your advice on both research as well as on my career have been priceless. I also would like to thank my co-supervisor Dr. Jagath Samarabandu for your help and advices during my graduate study period.

Besides my supervisors, I would like to thank the examiners from my thesis committee: Dr. Raveendra Rao, Dr. Liying Jiang and Dr. Weiming Shen, for coming for my thesis defence and helping me to improve my thesis quality.

I also would like to take this opportunity to express gratitude to all of the Department faculty members for their help and support.

I would like to thank my colleague, Dr. Aydin Behnad, Yu He and Kejun Tong for their help on my research.

Moreover, I would like to thank my research group, they not only give help on my research but also on my daily life. They are not only my colleagues but also my friends. Thanks to you guys for your support and accompany.

A special thanks to my family. Words can not express now grateful I am to my mother and father for all of the sacrifices that you have done on my behalf. I would also like to thank all of my friends who supported me in writing and encourage me to strive towards my goal.

Contents

List of Figures

List of Tables

List of Abbreviations

GPS	Global Positioning System
NLOS	None-Line-of-Sight
LBS	Location Based Service
RSS	Received Signal Strength
AoA	Angle of Arrival
ToA	Time of Arrival
TDoA	Time Difference of Arrival
AoA	Angle of Arrival
LoS	Line-of-Sight
FSPL	Free Space Path Loss
WLAN	Wireless Local Area Network
RSSI	Received Signal Strength Indicator
WiFi	Wireless Fidelity
INS	Inertial Navigation System
LSE	Least Square Estimation
MLE	Maximum Likelihood Estimation
CRLB	Cramér-Rao Lower Bound
MSE	Mean Square Error
MMSE	Minimum Mean Square Error

WSN	Wireless Sensor Network
WLSE	Weighted Least Square Error
SDR	Software-Defined Radio
FPGA	Field Programmable Gate Arrays
SoC	System on Chip
FMC	FPGA Mezzanine Card
RF	Radio Frequency
VGA	Variable Gain Amplifier
TX	Transimit
RX	Receive
MBDK	Model-Based Design Kit
ADC	Analog to Digital Converter
DAC	Digital to Analog Converter
JTAG	Joint Test Action Group
BSDK	Board Software Development Kit
CLI	Command Line Interface

Chapter 1

Introduction

1.1 Motivation

Over the last decades of years, localization and navigation have been recognized to play an increasingly important role in human society such as emergency rescue and social network applications. With fast development in wireless mobile networks and microelectronics technology, many smartphone-based applications, which require location information, have become more and more popular. These location information may include information from user device such as accelerations and orientation as well as information from base station such as signal strength. Location-based mobile applications in social networking services in our daily life such as Twitter, WeChat and Facebook, which allow users to share their locations and find nearby friends are attracting a lot of attention. Many content-aware applications in other fields also require location information in order to provide better services [1].

In the context of emergency services [2], locating victims and determining the best routes for rescue personnel are of vital importance as doing so saves power and time, which is essential in emergency scenarios. In the healthcare industry [3], real-time patient tracking can provide position prediction when other attempts to identify a location have failed.

The Global Positioning System (GPS)[4] is popular not only in the military but also in

day-to-day activities. However, GPS is only effective in outdoor environments as the building materials cause a lot of multipath situations known as None-Line-of-Sight (NLoS) situations. NLoS means there is significant multipath propagation or scattering due to a complex environment. In order to expand the application scenario, there has been a focus on indoor localization areas as well as joint localization fields.

To reduce the error of localization, improvements can be made in three parts: transmitters, receivers and the propagation process. Firstly, it is important to ensure that the information from the transmitters has being fully used. Efforts can be made to the optimum placement of base stations or reference nodes. In addition, rapid microelectronics development has motivated us to explore the solutions to minimize positioning errors with the help of built-in sensors from the receiver side such as the portable devices. Furthermore, the propagation process can be utilized to improve localization performance such as carrier frequency diversity.

In order to improve the localization performance from the first part, transmitters, many researchers have investigated into the reference node selection and placement[5]. All localization systems, such as ad-hoc networks and wireless sensors, need several reference nodes to locate and estimate the position of the target. Actually, the localization performance is in close relationship with the placement of the reference nodes[7][8]. As a result, the information from the reference nodes plays an important role in the localization process. It has been proved that the localization error is minimized when the reference nodes are placed uniformly[9]. However, this does not explain exactly where to place the reference nodes, especially in specific areas of interest. Thus, we are motivated to find the best placement for reference nodes within a specific area such that the average error is the lowest.

From the receiver side, since almost everyone in the world are using portable devices and many social applications are combined with positioning knowledge, a variety of discussions about the sensor utilization based on the smartphones have become popular. There are several embedded micro-electro-mechanical sensors in the portable devices collecting different types of data. The accelerometer sensor is the most common sensor used in the dead-reckoning

process. The authors in [10] make use of an accelerometer sensor to determine whether the user is stationary or moving. The sensor data is used as a filter since any acceleration causes large variation during the measuring process. In this case, the data from the accelerometer is not used fully, which motivates us to come up with a novel algorithm that combines the data output from the accelerometer and available anchors in its communication range to improve the localization performance.

A target can be positioning or tracking when people know how the signal propagates. The most widely used algorithm in this field is based on the received signal strength, as this saves the expense of adding specialized facilities. One of the popular methods, the radio map, relies on comparing the online signal strength with an offline recording. In [11], multiple frequencies and powers are recorded and selected to form a large fingerprint. Unfortunately, due to the complicated and varying surroundings, the radio map has to be updated frequently when used in indoor environments, otherwise significant errors may occur. On the other hand, accuracy will be affected as the frequency of the signal determines how the propagated signal is influenced by the surroundings. Due to the reasons above, we are motivated to explore the process of utilizing frequency diversity in indoor environment.

1.2 Research Objectives

The research objectives are to investigate the possibility of minimizing the localization error as well as improving the positioning performance, which can be divided into three different aspects: transmitter side, receiver side and signal propagation side.

Optimum Reference Nodes Placement: From the transmitter side, utilizing the information collected by the reference nodes for positioning has an obvious impact on the localization performance. Hence, the first research objective is to locate the reference nodes so as to improve the locating performance. According to the minimum mean square error, the optimum reference nodes placement is fixed. For more general situations, the deployment scheme is analyzed

over an area of interest with a random shape to set a certain number of reference nodes in it. Thus, the research objective is to minimize the average mean square error at the level of average localization.

Accelerometer Combined Localization: From the receiver side, the accelerometer sensor embedded in smartphones can be helpful when tracking a portable device. However, the accelerometer sensor accumulates measurement errors with time. As a result, we combine accelerations from accelerometer sensors with other localization technology such as received signal strength in order to decrease errors while tracking. The research objective here is to analyze the weighted least square error based on the joint localization system which combined localization information from accelerometer and available reference nodes.

Improved Positioning Using Frequency Diversity : From the signal propagation side, the frequency is a changeable parameter that can influence the path loss from the transmitter to the receiver. Investigating these impacts and making use of them is also a research objective herein. As frequency diversity leads to multi-channel measurements, which can be utilized to reduce the localization error, we propose a weighted scheme according to path loss fluctuation to improve the localization performance.

1.3 Contributions

The main contributions of this thesis are summarized below:

- An optimum reference node placement scheme to improve the localization performance is carried out in Chapter 3. The proposed algorithm can be implied in an arbitrary area with a set of reference nodes that is applicable in any real-world scenario. Instead of providing the best positioning result for a specific point, we offered the scheme that puts the reference node in the proper positions to present overall best results. As a result,

the positioning performance over a certain range is much better than when the reference nodes are placed randomly.

- A joint localization algorithm utilizing an embedded accelerometer sensor in the smartphone and available reference node in user's communication range is proposed in Chapter 4. The acceleration error is accumulates with time due to measurement error of the sensor. Based on weighted error minimization algorithm, tracking a user is achievable by combining the accelerometer information and available reference node information by assigning suitable weights to them.

- A frequency diversity-based positioning system is discussed in Chapter 5. The signal frequency information is applied instead of utilizing the reference nodes' position and distance information. Frequency diversity is investigated and different weights are assigned to frequency-based measurements according to path loss fluctuations to reduce the localization error thus to improve the positioning performance.

1.4 Thesis Outline

The rest of the thesis is organized as follows: In Chapter 2, we review the literature survey about localization technologies and examine some existing localization algorithms. In Chapter 3, the reference nodes placement scheme is presented according to minimum average mean square error over a certain region. In Chapter 4, we propose an algorithm to combine the location information from accelerometer with available reference nodes within its communication range. In Chapter 5, a frequency diversity-based localization scheme is proposed according to path loss fluctuations. We conclude our results and discuss future works in Chapter 6.

Chapter 2

Localization Techniques and Algorithms

Over the last few decades, localization has been a emerging topic in many fields, including healthcare, military and mobile applications. Mobile applications based on Location Based Services(LBSs) are becoming more and more popular, as the portable devices are everywhere in human society. LBSs can be defined as services that combines the location or position knowledge of the user with other information in order to provide better and more accurate services for a user[12]. As one of the most fundamental services in the LBSs, the localization of a node in a wireless network is valuable for enhancing the communication performance as well as achieving location-based services. Nevertheless, there are many challenges related to large-scale wireless network-based localization[13]. An immediate localization solution is to use the GPS. Of all the systems, technologies and platforms for localization, GPS is the most widely used as it provides comparatively good results. However, this approach fails in many scenarios because of the GPS signal blockage (e.g., indoor environments) or is not cost-effective when nodes are manufactured at a very large scale (e.g., wireless sensor networks). Due to this, localization results are not precise in many such situations. As a result, there has been extensive investigation into more practical and inexpensive localization methodologies. In this chapter, we will review some of the localization methods and systems.

2.1 Range Based Localization Technologies

According to [14], localization schemes can be divided into two general categories, range-based and range-free. Range-free schemes are defined as the situations where no direct measurement of range or angle is taken. This scheme can be grouped into two parts: local techniques, where the target is located by collecting information from neighbour anchors, and hop-count, where the distance between two nodes in range-free algorithm is expressed to be the sum of the smallest hops between a pair of nodes[5]. An earlier noticeable range-free positioning method called DV-Hop, which counts the hops from the target to the anchor in order to estimate the distances is presented in [6]. The range-free technique does not require any extra hardware. However, the range-free localization scheme is not accurate enough since it only uses proximity information.

In range-based localization schemes for indoor environments, there are generally three signal parameters based on which location of a target node and distances are determined: Received Signal Strength (RSS), Time of Arrival (ToA) or Time Difference of Arrival (TDoA), and Angle of Arrival (AoA)[15]. The RSS model works based on the fact that the transmitted signal is attenuated as a function of the distance between the target node and the reference transmitter. In ToA and TDoA, the signal propagation time between the pair of nodes (ToA) or the time difference of receiving the same transmitted signal by different nodes (TDoA) is measured and translated into distances. The AoA is based on the angular direction under which a signal is received and the distances are obtained using geometrical relations between the target node and reference nodes. RSS, AoA, and ToA/TDoA are the most common schemes in practical and have been extensively used for different localization scenarios[16].

2.1.1 Signal Strength-Based Localization

The signal strength-based localization technique does not require additional hardware as it utilizes a common feature found in most wireless devices. The path loss of signal while prop-

agating is calculated in the signal strength-based localization[17].

Signal fading in wireless communications

In wireless signal propagation, signals experience attenuation as a result of distance following the $1/d^2$ law in Line-of-Sight (LoS), where the receivers can be seen from the transmitter side (i.e., there is no obstacles between them). In NLoS, the signal is affected a lot by the surroundings. Three basic structures that affect signal propagation in NLoS are reflection, diffraction, and scattering. Reflection and diffraction happen when the propagating signal is obstructed by a smooth surface or a dense body, respectively. Scattering happens when the signal faces a rough surface. These situations are illustrated below in Figure 2.1.

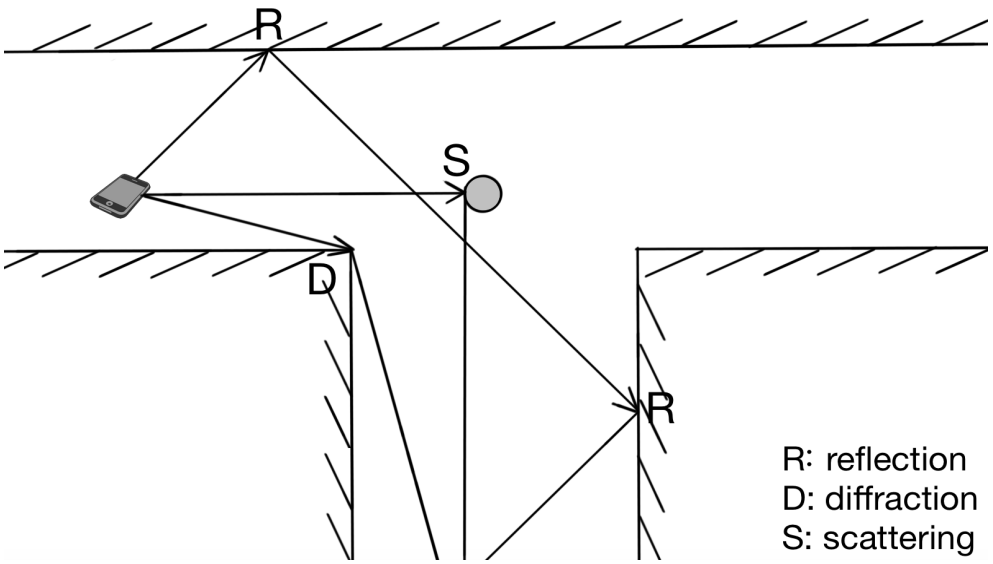

Figure 2.1: Illustration of reflection, diffraction and scattering.

Propagation path loss: This distance-dependent parameter is also called basic propagation loss. It can be modeled to be proportional to the inverse of the distance from the base station (i.e., $1/d^n$, where the exponent n is 2 in free space [18]). Free Space Path Loss (FSPL) is a measurement of how much the signal power drops from the transmitter to the receiver in a LoS

propagation which can be expressed as follows,

$$FSPL = (\frac{4\pi df}{c})^2, \tag{2.1}$$

where f is the signal frequency and c is the speed of light since propagation is always like light in free space. As the path loss is commonly expressed in unit of dB, Equation 2.1 can be written as

$$FSPL = -20log_{10}f(MHz) - 20log_{10}d(m) + 27.56, \tag{2.2}$$

$$FSPL = -20log_{10}f(MHz) - 20log_{10}d(km) + 32.45, \tag{2.3}$$

where $FSPL$ is the free space path loss measured in dB, f is the signal frequency measured in MHz and d are the distances measured in meters and kilometers respectively.

Shadowing: Shadowing is also called as slow fading or long-term fading. It is caused by the complex environment[19] and is normally distributed across an average value, which is usually assumed to follow a Gaussian distribution. Large-scale fading is shown in Figure 2.2. The path loss alone varies over a very long distance, usually between 100 and 1000 meters, while the variation due to shadowing happens when the distance is between 10 and 100 meters, which is proportional to the dimension of obstructions. As path loss and shadowing happen when the distance is relatively large, this kind of variation is usually called large-scale fading.

Multipath: Multipath fading is also called fast fading. The transmitted signal arrives at the receiver after reflection, diffraction, and scattering results in the multipath, which is significant in mobile communications as the mobile devices are usually at low heights and surrounded by obstacles. This small-scale fading is referred to as Rayleigh fading since there are various multipaths on at the receiver side with random amplitude and delay adding up to present a Rayleigh probability density function as a total signal. The red line in Figure 2.3 shows the fluctuations due to short-term fading.

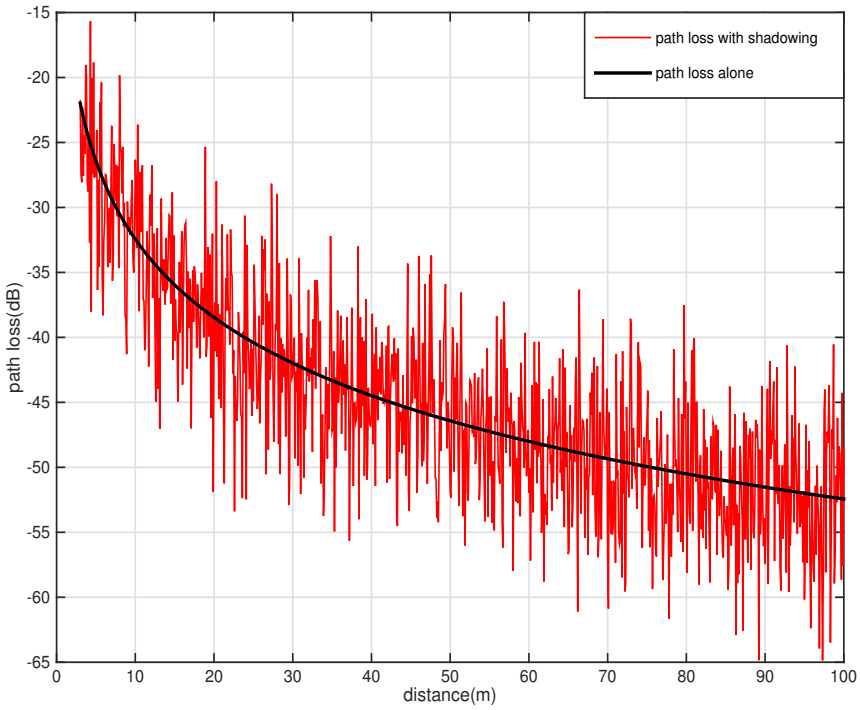

Figure 2.2: Path loss fading with shadowing.

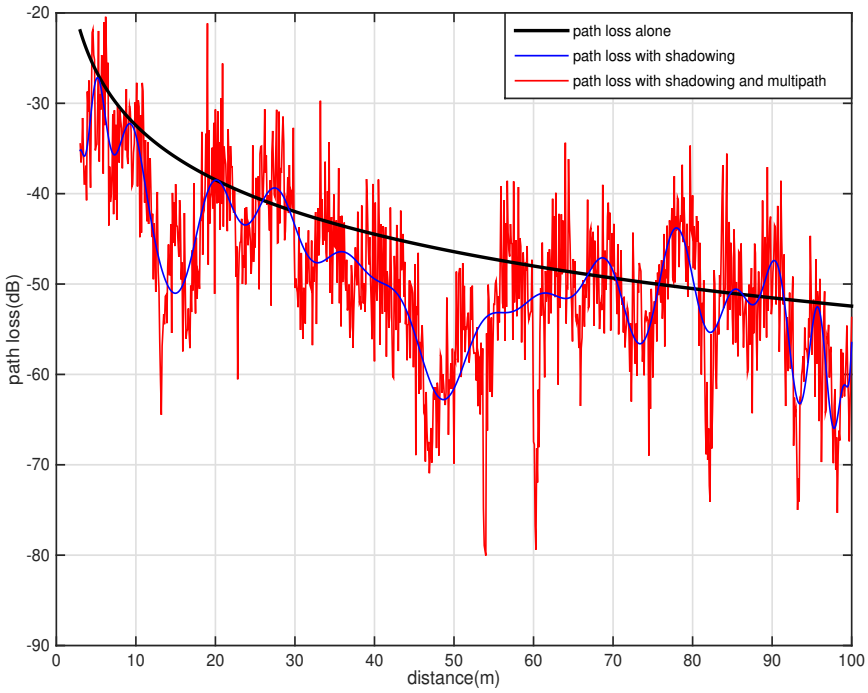

Figure 2.3: Path loss fading with shadowing and multipath fading.

Received Signal Strength Indicator technologies

Even though there are multiple options for the location-relating measurements such as ToA, TDoA, and AoA, RSS[20] is typically preferred for indoor Wireless Local Area Network (WLAN) localization due to its low expense and broad availability without the need for extra hardware.

Direct measurement: RSS is the simplest method of distance measurement based on the relation between the transmitted signal attenuation with distance; however, its accuracy is not good due to the multipath fading effect of the environment. Also the positioning error is a multiplicative factor of the range and increases proportional to the distance[21].

Received Signal Strength Indicator (RSSI) is a convenient and low-cost option for localization systems as most transceiver hardware is equipped with it[22][23]. Plenty of research has been done to investigate the relationship between the power and distance[40]. In many experimental findings, the distance follows a power law. In free space propagation models, the ratio between the transmitted signal power and the received signal power can be expressed as

$$\frac{P_r}{P_t} = \frac{G_t G_r \lambda^2}{(4\pi d)^2}, \tag{2.4}$$

where P_r is the power of the received signal, P_t is the power of the transmitted signal, G_r is the antenna gain of the receiver, G_t is the antenna gain of the transmitter, and d is the distance between the receiver and transmitter.

But in reality, as a result of the influence from obstacles, the path loss tends to obey a log-normal-shadowing model as below

$$P(d) = P(d_0) - 10nlog(\frac{d}{d_0}) + \sigma, \tag{2.5}$$

where $P(d_0)$ is the reference path loss at the reference distance d_0 from the receiver to the transmitter. d_0 is commonly defined as 1 meter and $P(d_0)$ is the corresponding path loss. $P(d)$

is the path loss at the target point when it has a distance of d from the transmitter; n is the path loss exponent, which is usually between 2 and 5; and σ is usually a Gaussian random variable with zero mean, which reflects the attenuation due to fading.

In the embedded devices, the received signal strength is transferred to the RSS instead. The definition is

$$RSS = 10 \cdot log(\frac{P_r}{P_{ref}}), \tag{2.6}$$

where P_{ref} is usually defined as $1mW$ and P_r is the received signal strength.

Fingerprinting: While the above localization technique is based on the real-time measurement to derive the distance, the fingerprinting technology relies on observations attempting to match real-time measurements. As it is well known that a lot of work should be done prior to operation as well as repeated work if the environment changes, this RSS fingerprinting provides better accuracy than direct RSS estimation[41][42]. The Microsoft Research RADAR location system is an application for the fingerprinting based on the Wireless Fidelity (WiFi) signal strength for indoor environments[43]. In indoor localization, GSM signal strength can also be used to build a RSS map[44]. The RSS values for one position are recorded from all of the nearby anchors in its communication range.

This technology usually involves a two-step process.The first step is offline or the learning phase, the RSS measurements at different positions are recorded. During this stage, the mobile nodes are usually held by testers and the anchor nodes record the power level of the signal strength from the mobile nodes to set up the RSS map. The second step is an online phase and occurs after the database has been built in the previous stage. The signal strengths are compared to find the best match between the observed signal strength and the recorded signal strength.

The drawback of the fingerprinting technology is its high expense, which is generally due to the build up labour as well as the large database.

2.1.2 Time Based Localization

Various accurate localization systems make use of the measurements of signal travel time, as this technology can reach centimeter-level accuracy.

Time of Arrival: The ToA technique is more complex than the RSS technique but the resulting measurement errors are less multiplicative. Time measurement using ToA is usually more accurate than signal strength-based localization technology, as RSS is significantly affected by obstacles and walls.

ToA calculates the distance between the reference and target nodes by computing the traveling time between them. The distance between two nodes is proportional to the travel time of the signal from one node to another[30]. Let t denotes the time when the target point is at (x, y) as t_r denotes the time when the reference point position is (x_r, y_r). Since the speed of the wireless signal in air is the same as the light c, the distance d between them can be computed by[26]

$$d = (t_r - t_0)c. \tag{2.7}$$

However, the transmitter and receiver in ToA systems must be synchronized, which is difficult to achieve[27].

Time Difference of Arrival: The above ToA technology requires complete synchronization between the target point and the reference node, which is not possible in reality. As a result, TDoA can be an alternative method used to lower the influence of non-synchronization.

Generally, the TDoA estimation method is used to measure the time difference of the signal from the target arriving at different base stations, as illustrated in Figure 2.4. This method utilizes the fact that the points in the hyperbola have different constant distances to two fixed points in the plane[25]. As a result, the target must be on the hyperbola. Usually two or more sets of hyperbolas or at least three base stations will be needed to locate the target. As a result, the two base stations must be synchronized well. The advantage is that when the

channel characteristics of the base stations are similar, the error caused by the multipath can be reduced.

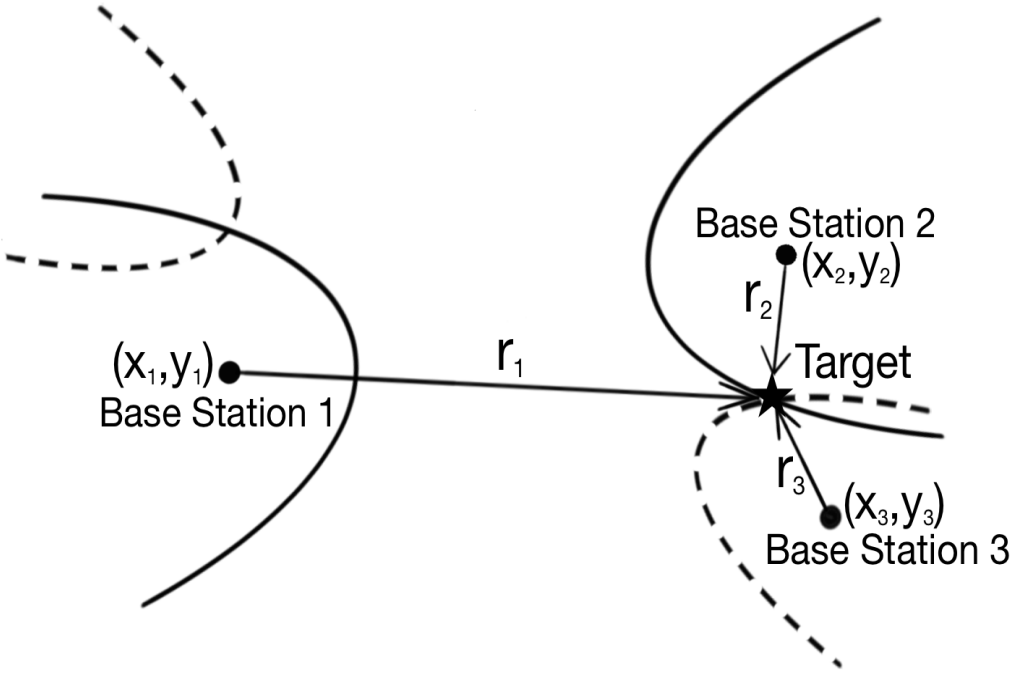

Figure 2.4: Estimated localization based on TDoA technology

TDoA achieves accurate results and is widely used in localization systems such as GPS[28] and television[29]. However, this technique requires additional hardware to perform time measurements.

2.1.3 Angle Based Localization

The AoA scheme is more complicated and is also affected by the multipath fading effect. AoA technology requires at least two base stations[30] and locates the target at the intersection, as shown in Figure 2.5. Directional antenna or antenna array are used to make the angular measurements in AoA-based localization systems[31].

The advantage of AoA is that it does not require any synchronization between the antennas. Also, AoA estimation can be determined with only two base stations for 2D localization or three for 3D localization. However, it can cause more errors when obstacles increase due to

the multipath. There are limitations, as AoA cannot reach long distances, which is a result of large distance errors caused by angular resolution.

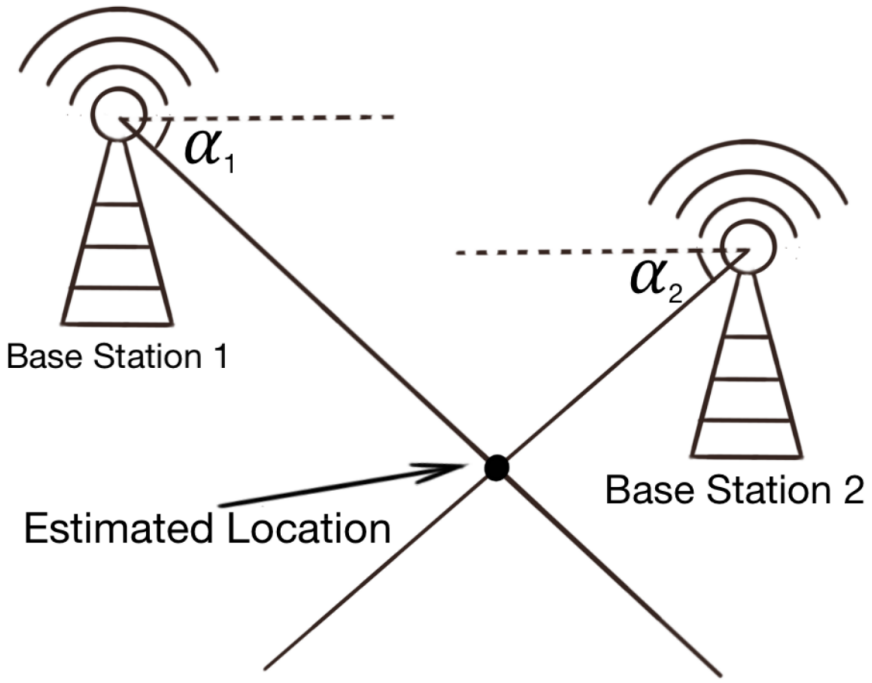

Figure 2.5: Estimated localization based on AoA technology

2.2 Localization Estimation Algorithms

The localization of an object in reality is estimated by requiring some physical measurements based on its characteristics using localization technologies such as the ones discussed in the last section. However, the localization information collected by above localization technologies is not accurate on its own. Depending on the localization information from measurements, there is a variety of algorithms which can be used to narrow the localization error.

2.2.1 Least square estimation

In wireless localization estimation systems, one of the most widely used methods is the Least Square Estimation (LSE) method. It is published in [32] for the first time and after several

developments[33] it is clearly and concisely written in [34]. LSE is to fit a line that has the minimal sum of squared deviation compared to a collection of existing data.

Suppose we have a user whose position is denoted by (x, y) and a base station denoted by $(x_i, y_i), i = 1, 2, ..., N$. In the first localization step, the real distance between the user and base station d_i can be expressed as

$$d_i = \sqrt{(x - x_i)^2 + (y - y_i)^2}. \tag{2.8}$$

However, in range measurement, the distances usually come with an ranging error:

$$\hat{d}_i = d_i + e_i, \tag{2.9}$$

where e_i demonstrates the error caused by the RSS, ToA or AoA measurements. As a result, the Equation 2.8 should be written as

$$(x - x_i)^2 + (y - y_i)^2 = \hat{d}_i^{\,2}. \tag{2.10}$$

Expanding Equation 2.10, we get

$$-2x_i x - 2y_i y + x^2 + y^2 = \hat{d}_i^{\,2} - x_i^2 - y_i^2. \tag{2.11}$$

Using the linear least squares method, if we present it in matrix form, we can get

$$\mathbf{A}\mathbf{\Lambda} = \mathbf{b}, \tag{2.12}$$

where $\mathbf{A} = \begin{pmatrix} -2x_1 & -2y_1 & 1 \\ -2x_2 & -2y_2 & 1 \\ \vdots & \vdots & \vdots \\ -2x_N & -2y_N & 1 \end{pmatrix}$, $\mathbf{\Lambda} = \begin{pmatrix} x \\ y \\ x^2 + y^2 \end{pmatrix}$ and $\mathbf{b} = \begin{pmatrix} \hat{d}_1^{\,2} - x_1^2 - y_1^2 \\ \hat{d}_2^{\,2} - x_2^2 - y_2^2 \\ \vdots \\ \hat{d}_N^{\,2} - x_N^2 - y_N^2 \end{pmatrix}$.

However, when N is large, the estimator is overdetermined and will have more than one solution for $\mathbf{A\Lambda} = \mathbf{b}$. The solution of the least square problem is presented as follows:

$$(x, y) = \arg\min_{(x,y)} \|\mathbf{A\Lambda} - \mathbf{b}\|^2. \tag{2.13}$$

Then, the solution $\mathbf{A\Lambda} \approx \mathbf{b}$ can be expressed as

$$\mathbf{A}^T\mathbf{A\Lambda} = \mathbf{A}^T\mathbf{b}, \tag{2.14}$$

$$\mathbf{\Lambda} = (\mathbf{A}^T\mathbf{A})^{-1}\mathbf{A}^T\mathbf{b}. \tag{2.15}$$

Compared to Maximum Likelihood Estimation (MLE), which will be discussed in the following section, LSE is a sub-optimum localization algorithm. However, it is simpler than MLE and provides a comparatively accurate output since it does not demand iterative calculations and has a closed-form result.

2.2.2 Maximum likelihood estimation

MLE is a relatively simple method of estimating the parameters of a statistical model given data. MLE can be applied to most problems and is one of the earliest techniques investigated in the localization problems, since MLE technology is perhaps the most recognized estimation method in statistics. It is widely recommended by Ronald Fisher[35] followed by several developments from other authors. The aim of MLE technology is to maximize the probability of the observed data that is independent under a certain distribution. If the sample is large enough, this statistic method will act as an effective estimator.

Assume there is a set of random samples x_1, x_2, ..., x_n of n independent and identical distributions $f(x_1|\theta)$, $f(x_2|\theta)$, ..., $f(x_n|\theta)$, which are probability density functions. Here, the given symbol indicates that the distribution is dependent on a parameter θ, which could be a real-valued unknown parameter or a vector of parameters. The joint density function for a set

of independent and identically distributed random variables is

$$f(x_1, x_2, ..., x_n|\theta) = f(x_1|\theta) \times f(x_2|\theta) \times ... \times f(x_n|\theta). \tag{2.16}$$

We call $f(x_1, x_2, ..., x_n|\theta)$ the likelihood function and it is always denoted as $L(\theta)$. MLE attempts to maximize the likelihood function $L(\theta)$ with respect to the unknown parameter θ. $L(\theta)$ is equivalent to $logL(\theta)$ as log is a monotonic increasing function. $logL(\theta)$ is called log likelihood function and is denoted as $l(\theta)$ as follows:

$$l(\theta) = logL(\theta) = log \prod_{i=1}^{n} f(x_i|\theta) = \sum_{i=1}^{n} log f(x_i|\theta). \tag{2.17}$$

In a localization problem, the distance measurement D_i between the target T and the anchor R_i is a random variable following Gaussian distribution $N(\mu_i, \sigma^2)$ where μ_i is the actual distance between the unknown node T and the ith reference node R_i. σ^2 is usually set to be a fixed constant. Suppose the range measurements are independent from each other and let the sample value be $d_i, i = 1, 2, ..., N$.

The probability density functions of D_i are

$$f_i(x) = \frac{1}{\sqrt{2\pi}\sigma} e^{-\frac{(x-\mu_i)^2}{2\sigma^2}}, \tag{2.18}$$

where the real distance $\mu_i = \sqrt{(x_i - x)^2 + (y_i - y)^2}$. In this way, the MLE likelihood function is presented below:

$$\begin{aligned} L(x, y) &= \prod_{i=1}^{N} f_i(d_i) = \prod_{i=1}^{N} \frac{1}{\sqrt{2\pi}\sigma} e^{-(d_i - \mu_i)^2/2\sigma^2} \\ &= \left(\frac{1}{\sqrt{2\pi}\sigma}\right)^N e^{-1/2\sigma^2 \sum_{i=1}^{N} (r_i - \mu_i)^2}. \end{aligned} \tag{2.19}$$

In the MLE localization process, the aim is to maximize the likelihood function $L(x, y)$, which is equivalent to maximizing $logL(x, y)$. As $logL(x, y)$ is more simple and straightforward

to solve, here we derive it as follows:

$$l(x,y) = logL(x,y) = Nlog(\frac{1}{\sqrt{2\pi}\sigma}) - \frac{1}{2\sigma^2}\sum_{i=1}^{N}(r_i - \mu_i)^2. \tag{2.20}$$

Maximizing Equation 2.20 is to minimize $u(x,y) = \sum_{i=1}^{N}(r_i - \mu_i)^2/(2\sigma^2)$, which is equal to figuring out the equation set below:

$$\begin{aligned} \frac{\partial u}{\partial x} &= \sum_{i=1}^{N}(x_i - x)\frac{\mu_i - r_i}{\mu_i} = 0, \\ \frac{\partial u}{\partial y} &= \sum_{i=1}^{N}(y_i - y)\frac{\mu_i - r_i}{\mu_i} = 0. \end{aligned} \tag{2.21}$$

By solving the localization problem using the MLE technology outlined above, the accuracy can be increased compared to when the multilateral range measurement information in linear least square method is used. MLE attains the lower bound when the sample amount N goes to infinity.

2.2.3 Cramér-Rao Lower Bound

Cramér-Rao Lower Bound (CRLB) provides a lower bound on the variance of the estimator whose name is in honor of authors who derive it[36][37].

After obtaining the *log* likelihood function, we also have information about other parameters related to the MLE technique. The score function is the one simply present in the gradient of *log* likelihood:

$$s(\boldsymbol{\theta}) = \frac{\partial logL(\boldsymbol{\theta})}{\partial \boldsymbol{\theta}}, \tag{2.22}$$

where we set $\boldsymbol{\theta} = (x, y)$ as the unknown parameter in the location estimation problem and $L(\boldsymbol{\theta})$ is the likelihood function, which is also the joint density function $f(\boldsymbol{X}; \boldsymbol{\theta})$, where $\boldsymbol{X} : (x_i, y_i), i = 1, 2, ..., N$ is the observable random variable.

The Fisher information (sometimes simply called the information), which is denoted as

$\mathbf{I}(\boldsymbol{\theta})$, is defined as the matrix of the second moments of the score function[50]:

$$\mathbf{I}(\boldsymbol{\theta}) = E[s^2(\boldsymbol{\theta})] = E\left[\left(\frac{\partial logL(\boldsymbol{\theta})}{\partial \boldsymbol{\theta}}\right)^2\right]. \tag{2.23}$$

The Fisher information can also be expressed as

$$\mathbf{I}(\boldsymbol{\theta}) = -E\left[\frac{\partial^2 logL(\boldsymbol{\theta})}{\partial^2 \boldsymbol{\theta}}\right] \tag{2.24}$$

since

$$\begin{aligned} E\left[\frac{\partial^2 logL(\boldsymbol{\theta})}{\partial^2 \boldsymbol{\theta}}\right] &= E\left[\frac{\partial}{\partial \boldsymbol{\theta}}\left(\frac{1}{L(\boldsymbol{\theta})}\frac{\partial logL(\boldsymbol{\theta})}{\partial \boldsymbol{\theta}}\right)\right] \\ &= E\left[\frac{1}{L(\boldsymbol{\theta})}\cdot\frac{\partial^2 L(\boldsymbol{\theta})}{\partial \boldsymbol{\theta}^2} - \left[\frac{1}{L(\boldsymbol{\theta})}\frac{\partial L(\boldsymbol{\theta})}{\partial \boldsymbol{\theta}}\right]^2\right] \\ &= \int \frac{1}{L(\boldsymbol{\theta})}\cdot\frac{\partial^2 L(\boldsymbol{\theta})}{\partial \theta^2}\cdot L(\boldsymbol{\theta})d\boldsymbol{\theta} - E\left[\left(\frac{\partial logL(\boldsymbol{\theta})}{\partial \boldsymbol{\theta}}\right)^2\right] \end{aligned} \tag{2.25}$$

and the first moment of the score which is the expectation of the score is 0:

$$\begin{aligned} \int \frac{1}{L(\boldsymbol{\theta})}\cdot\frac{\partial^2 L(\boldsymbol{\theta})}{\partial \theta^2}\cdot L(\boldsymbol{\theta})d\boldsymbol{\theta} &= \int \frac{\partial^2 L(\boldsymbol{\theta})}{\partial \theta^2}d\boldsymbol{\theta} \\ &= \frac{\partial^2}{\partial \theta^2}\int L(\boldsymbol{\theta})d\boldsymbol{\theta} \\ &= \frac{\partial^2}{\partial \theta^2}\cdot 1 = 0, \end{aligned} \tag{2.26}$$

Thus, the Fisher information is also called the variance of the score.

Now, we know that $\boldsymbol{X}$ is a vector of random variables $(x_i, y_i), i = 1, 2, ..., N$ and the joint density function is $f(\boldsymbol{X}; \boldsymbol{\theta})$ where $\boldsymbol{\theta}$ is the target location (x, y) in the localization problem. The CRLB indicates that the inverse of the Fisher information is a lower bound on the variance of

any unbiased estimator of $\boldsymbol{\theta}$. The Cramér-Rao inequality is

$$Var[\boldsymbol{\theta}(\boldsymbol{X})] \geq \frac{1}{\boldsymbol{I}(\boldsymbol{\theta})}, \tag{2.27}$$

where $\boldsymbol{I}(\boldsymbol{\theta})^{-1}$ is the CRLB. This inequality tells us that in the localization problem the precision to which we can estimate the target $\boldsymbol{\theta} : (x, y)$ is basically limited by the Fisher information.

2.3 Sensor Measurements

Smartphones not only provide provide RADAR and GPS but also offer a variety of Inertial Navigation System (INS) sensors, such as accelerometer, magnetometer, gyroscope, whose information can be used to locate the portable devices. These sensors present useful information to locate and track users.

2.3.1 Accelerometer

In instances of acceleration of the device, the accelerometer can not only be used to locate a target, but also can be analyzed to detect the activities of the user. Almost all recent smartphones have three-axial accelerometers, making them a good choice for pedestrian dead reckoning and locating users. Accelerometers can help detect human activities such as going upstairs or downstairs and walking which is ideal for patients detection in medical field. In addition, accelerometer values can be used for calculating the velocity and location of a robot[39].

However, the accelerometer itself has measurement error. The direct evidence is that while placing a smartphone on a desk or keeping it static in hand, the sensor will report the smartphone is moving. Although the readings from accelerometer along three axes are small, it can accumulate to a large error with time. Efforts have been done due to this weakness. One of them is to record the accelerations only when it is above a certain threshold.

2.3.2 Magnetometer

Magnetometer measures the earth's magnetic field strength. Magnetic field sensors' directions are determined with respect to the North Magnetic Pole on the surface of the Earth and the unit used is microtesla (μT). Compass is one of the application based on this feature which can give orientation of the user. However, this sensor is very sensitive to the surroundings such as electronic devices or buildings materials, which can be regarded as noise. It has been revealed in [38] that disturbances of the magnetic field can be utilized to locate the users.

2.3.3 Gyroscope

Gyroscopes are used to assist the magnetometer as well as the accelerometer to increase the precision of localization. Radians per second (rad/s) are measured using the gyroscope sensor, which shows the difference of the smartphones' rotation, namely, the angular velocity. Even though the magnetic field sensor is slower than the gyroscope, the gyroscope can only be utilized to assist with the magnetometer for higher precision since, unlike the magnetometer, the gyroscope cannot determine the orientation of the phone. Thus, a combination of these motion sensors can provide an overall good performance since the magnetic field sensor offers long-term information while the gyroscope provides quick adjustments to the short-term data.

2.4 Chapter Summary

In this chapter, we review the techniques and algorithms used in localization system. Positioning techniques are classified into two categories, range-based and range-free schemes. Range-based localization technologies, including signal-based, time-based and angle-based technologies, are discussed first. LSE and MLE are both regression estimation methods used to minimize the error of localization and maximize the probability of measurements respectively; they are also analyzed in details. Estimator based on CRLB is another algorithm that can be used to provide the lower bound of variance. Smartphone sensors are investigated in the

end to give a general view on INS sensors which can provide additional assistance to localization techniques and algorithms.

Chapter 3

Optimum Reference Node Deployment for Indoor Localization Based on the Average Mean Square Error Minimization

Considering all the localization systems, a critical common issue needs to be tackled is to determine the physical positions of reference nodes. In [24], it shows that the placement of reference nodes has substantial impact on the positioning accuracy. Therefore, finding the optimum locations for reference nodes are vital in nearly every localization systems and reference nodes placement strongly affects the quality of localization. In this chapter, average mean square error is minimized to obtain best average localization performance over certain regions.

3.1 Introduction

Many localization methods proposed have been proposed recently to find the optimum reference nodes to reduce the localization estimation error. In [45], reference anchors are optimized to improve the performance of linear least squares and weighted least squares algorithm in RSS-based localization.

Using the GPS for indoor localization is challenging as the GPS signal is significantly attenuated or completely blocked by the building. In achieving indoor localization, a set of transmitters from wireless communication networks are often used as reference nodes to localize target nodes with unknown locations. The accuracy of such localization process is considerably affected by the spatial distribution of the reference nodes with respect to the target node to be localized. Hence, deploying the reference nodes at best locations will notably increase the localization precision. In this chapter, a novel reference nodes deployment scheme is introduced which minimizes the average Mean Square Error (MSE) of the localization over the area of interest with certain shape. The proposed scheme is evaluated for deploying the reference nodes in the circular, square, and hexagonal localization regions. The proposed scheme is validated and illustrated by numerical simulations.

In wireless networks, CRLB is usually defined as a benchmark so that we can know how good an estimator will possibly do[13]. It also helps us compare the performances between different localization estimations[46]. Average CRB is derived in [21] based on RSS localization to study the nonlinear least square solution presented. Another ToA-based average CRLB in NLoS environment can be found in [47]. According to [47] and [48], CRLB provides a lower bound on the MSE of a position estimate. In some cases, average MSE is used to evaluate practical estimators' performance in positioning systems. A reference node selection strategy is proposed in [49] which minimizes the average MSE in the TDoA based position system. In this paper, we are interested in the first two diagonal terms of the CRLB which provide the Minimum Mean Square Error (MMSE) of the position estimation. We propose a reference nodes deployment scheme which determines the optimum locations by minimizing MMSE over selected areas which can be circle, hexagon or square. Besides, our scheme can also be used as the guidance for deploying reference nodes in localization system.

3.2 Minimum Mean Square Error Scheme

As mentioned above, ToA is based on the signal propagation time measurement between nodes. If (x_T, y_T) is the location of a target node T being localized and (x_i, y_i) is the location of the i-th reference node localizing T,

$$d_i(x, y) = \sqrt{(x_T - x_i)^2 + (y_T - y_i)^2} \tag{3.1}$$

is the distance between T and the i-th reference node. In this case, the signal propagation time is measured as

$$t_i = \frac{d_i}{c} + \zeta_i, \quad i = 1, ..., N, \tag{3.2}$$

where constant c is the signal propagation speed, and ζ_i is the measurement noise which is usually modeled as a zero-mean Gaussian random variable with a constant variance σ_i^2[13], and N is the number of reference nodes. In this case, the location of T is obtained based on the measured time values $(t_1, t_2, \ldots, t_N)$. In addition, if $(\hat{x}_T, \hat{y}_T)$ is the estimated location of T, then the localization error is obtained as

$$e = \sqrt{(\hat{x}_T - x_T)^2 + (\hat{y}_T - y_T)^2}, \tag{3.3}$$

which can be used to compare the accuracy between different localization estimators.

In addition to the accurate estimation of the distances between the target node and any of the reference nodes, the topology of the reference nodes with respect to the target node can also significantly affect the performance of the target node localization. Hence, in order to get the best estimation of the target node, it is more efficient to use the reference nodes with optimum locations for locating the target node.

The average mean square error of e derived in (3.3) is a good figure of merit to select the best set of the reference nodes for the localization. Using a CRLB approach, it has been shown

in [47] and [48] that the MMSE of the ToA localization scheme is given by

$$MMSE_{ToA} = \frac{c^2 \Sigma_{i=1}^{N_L} \sigma_i^{-2}}{\Sigma_{i=1}^{N_L} \Sigma_{j=1}^{i-1} \sigma_i^{-2} \sigma_j^{-2} \sin^2(\theta_i - \theta_j)}, \tag{3.4}$$

where c is the speed of the light, σ_i and σ_j represent the ith and jth ToA measurement errors respectively, N_L is the number of reference nodes. $\theta_i = \tan^{-1}(\frac{y-y_i}{x-x_i})$ and it denotes the angle between the ith reference node and the target node. (x, y) and (x_i, y_i) are the positions of the target node and the ith reference node, respectively.

In order to get the average MMSE within a certain range, we have to get the average MMSE expression. The ToA-based average MMSE result can be expressed as

$$MMSE(x, y) = \frac{c^2 \sigma^2 N}{\sum_{i=1}^{N-1} \sum_{j=i+1}^{N} (\sin \theta_{ij})^2}, \tag{3.5}$$

where $\theta_{ij} = \theta_i - \theta_j$ and N is the number of reference nodes. σ^2 denotes the ToA measurement error.

In the usual situation where has 3 reference nodes , we can simplify the average MMSE expression from (3.5) to

$$MMSE(r, \theta) = \frac{3c^2 \sigma^2}{\sin^2 \theta_{12} + \sin^2 \theta_{23} + \sin^2 \theta_{13}}, \tag{3.6}$$

where θ_{12}, θ_{23} and θ_{13} denote the angular distances between every two reference nodes as shown in Figure 3.1. The target node is in the center of the figure presented as triangle and the 3 reference nodes are randomly distributed which are circles in Figure 3.1. In this paper, we set $c\sigma$ equal to 1. Also, $\sin^2 \theta_{12}$, $\sin^2 \theta_{23}$, $\sin^2 \theta_{13}$ can be derived by the vector product expression

$$\mathbf{a} \times \mathbf{b} = \| \mathbf{a} \| \cdot \| \mathbf{b} \| \sin \theta, \tag{3.7}$$

where $\mathbf{a}$ and $\mathbf{b}$ are the vectors of segments connect the target node and the reference node.

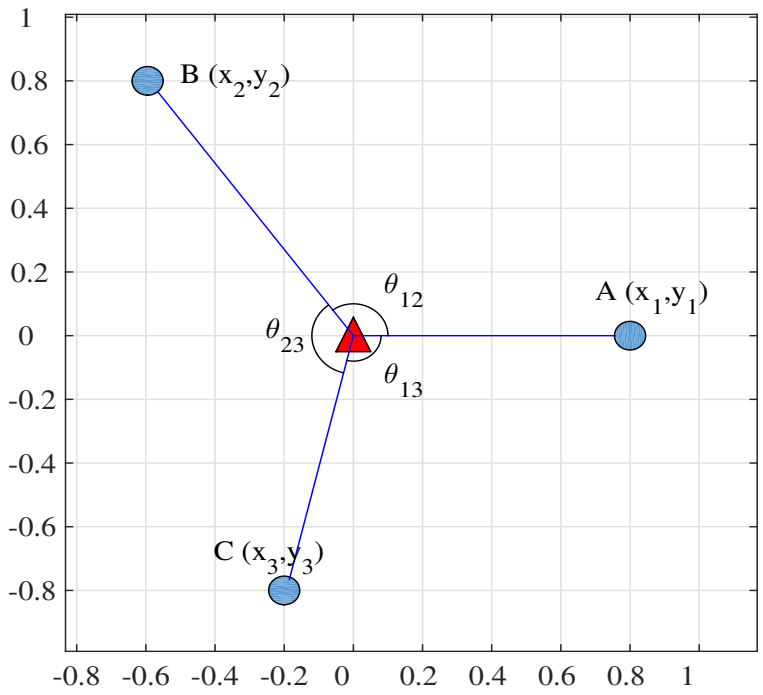

Figure 3.1: Illustration of 3 Reference Nodes in the Mean Square Error Minimization Problem

3.3 Average Scheme In Certain Localization Regions

We consider a three-reference-node localization scenario to localize a target node T located in a determined localization region. We analyze three different cases separately. In the first case, one reference node is assumed to be fixed at the center of the localization region, which with refer to it as the base station, whereas the other two nodes are deployed to help the base station to localize T which minimize the localization error over this region.

At first, we assume the nodes are in an unit circle. In this circular region, there are one reference node O with known location in the center and two reference nodes A, B with unknown location within the circle, then the parameters in average MMSE expression from (3.6) can be calculated out as

$$\sin^2\theta_{12} = \frac{r_A^2 \sin^2\theta}{r_A^2 + r^2 - 2rr_A\cos\theta}, \tag{3.8}$$

$$\sin^2\theta_{23} = \frac{(rr_B\sin(\theta-\theta_0) - rr_A\sin\theta + r_Ar_B\sin\theta_0)^2}{(r^2 + r_B^2 - 2rr_B\cos(\theta-\theta_0))(r_A^2 + r^2 - 2rr_A\cos\theta)} \tag{3.9}$$

and

$$\sin^2\theta_{13} = \frac{r_B^2 \sin^2(\theta - \theta_0)}{r^2 + r_B^2 - 2rr_B\cos(\theta - \theta_0)}. \tag{3.10}$$

Here, r_A and r_B are the distances between O and A, B respectively. r is the distance between T and O. θ is the angular distance between the segments which connect A, T with O. θ_0 denotes the angular distance between the segments which connect A, B with O.

The average MMSE result within this unit circle is considered as

$$\overline{MMSE} = \frac{1}{\pi}\int_0^{2\pi}\int_0^1 MMSE(r,\theta|r_A,r_B,\theta_0)rdrd\theta. \tag{3.11}$$

In this way, the optimum locations of reference nodes A, B can be obtained by minimizing the average MMSE expression.

$$(\hat{r}_A,\hat{r}_B,\hat{\theta}_0) = \text{argmin}\,\overline{MMSE} \tag{3.12}$$

In this case, we also consider the square region as well as the hexagonal region to prove the flexibility of our scheme. For these two regions, the parameters of average MMSE expression in (3.6) are (3.13), (3.14) and (3.15).

$$\sin^2\theta_{12} = \frac{(x_Ay_C - x_Cy_A)^2}{(x_C^2+y_C^2)(x_A^2+x_C^2-2x_Ax_C+y_C^2+y_A^2-2y_Ay_C)}, \tag{3.13}$$

$$\sin^2\theta_{23} = \frac{(x_By_C + x_Ay_B + x_Cy_A - x_By_A - x_Ay_C - x_Cy_B)^2}{(x_B^2+x_C^2-2x_Bx_C+y_C^2+y_B^2-2y_By_C)(x_A^2+x_C^2-2x_Ax_C+y_C^2+y_A^2-2y_Ay_C)}, \tag{3.14}$$

$$\sin^2\theta_{13} = \frac{(x_By_C - x_Cy_B)^2}{(x_C^2+y_C^2)(x_B^2+x_C^2-2x_Bx_C+y_B^2+y_C^2-2y_By_C)}. \tag{3.15}$$

The average MMSE expression within a square whose side is 1 is as follow:

$$\overline{MMSE} = \int_{-\frac{1}{2}}^{\frac{1}{2}}\int_{-\frac{1}{2}}^{\frac{1}{2}} MMSE(x_C,y_C|x_A,y_A,x_B,y_B)dxdy. \tag{3.19}$$

Similarly, the average MMSE expression within a hexagon whose side is 1 is as follow:

$$\begin{aligned}\overline{MMSE} = \frac{2\sqrt{3}}{9}\int_{-\frac{\sqrt{3}}{2}}^{\frac{\sqrt{3}}{2}}\int_{-1}^{1} MMSE(x_C, y_C|x_A, y_A, x_B, y_B)dxdy \\ -4\int_{-\frac{\sqrt{3}}{2}}^{0}\int_{-\frac{\sqrt{3}}{2}}^{-\frac{\sqrt{3}}{3}x-1} MMSE(x_C, y_C|x_A, y_A, x_B, y_B)dxdy.\end{aligned} \tag{3.20}$$

By minimizing the average MMSE result, we can get the positions of optimum reference nodes by

$$(\hat{x}_A, \hat{y}_A, \hat{x}_B, \hat{y}_B) = \text{argmin}\,\overline{MMSE} \tag{3.21}$$

in square region or in hexagonal region.

In the second case, we consider a situation where there are two reference nodes A and B with known location at central axis of a region. In circular region, we set A to (1,0) or ($\frac{1}{3}$,0) and B to (-1,0) or (-$\frac{1}{3}$,0) respectively. C is the reference node with unknown location within the region that we want to obtain. In this assumption, the parameters in (3.6) are

$$\sin^2\theta_{12} = \frac{(rr_B\sin\theta - rr_A\sin\theta)^2}{(r_A^2 + r^2 - 2rr_A\cos\theta)(r_B^2 + r^2 - 2rr_B\cos\theta)}, \tag{3.22}$$

$$\sin^2\theta_{23} = \frac{(r_Ar_C\sin\theta_0 - rr_A\sin\theta + rr_C\sin(\theta-\theta_0))^2}{(r^2 + r_C^2 - 2rr_C\cos(\theta-\theta_0))(r_A^2 + r^2 - 2rr_A\cos\theta)}, \tag{3.23}$$

and

$$\sin^2\theta_{13} = \frac{(r_Br_C\sin\theta_0 - rr_B\sin\theta + rr_C\sin(\theta-\theta_0))^2}{(r_B^2 + r^2 - 2rr_B\cos\theta)(r^2 + r_C^2 - 2rr_C\cos(\theta-\theta_0))}. \tag{3.24}$$

Similarly, in square and hexagonal region, the parameters in (3.6) are

$$\sin^2\theta_{12} = \frac{(x_By_C - x_By - xy_C + x_Cy)^2}{[(x_B - x)^2 + y^2][(x_C - x)^2 + (y_C - y)^2]}, \tag{3.25}$$

$$\sin^2\theta_{23} = \frac{(x_Ay_C - x_Ay - xy_C + x_Cy)^2}{[(x_A - x)^2 + y^2][(x_C - x)^2 + (y_C - y)^2]} \tag{3.26}$$

and

$$\sin^2\theta_{13} = \frac{(x_A y - x_B y)^2}{(x_B^2 + x^2 - 2xx_B + y^2)(x_A^2 + x^2 - 2xx_A + y^2)}. \tag{3.27}$$

But in hexagonal region, A and B are set to be $(\frac{\sqrt{3}}{6}, 0)$ and $(-\frac{\sqrt{3}}{6}, 0)$ or $(\frac{\sqrt{3}}{2}, 0)$ and $(-\frac{\sqrt{3}}{2}, 0)$.

Actually in reality, there is no reference node with known location in advance for many cases. So at last, we consider the third case where we want to obtain three reference nodes A, B and C without prior location information. We present the parameters in (3.6) as (3.28), (3.29) and (3.30) in circular region where θ_A, θ_B, θ_C, θ_T denote the angle between the x-axis through the center of the circle and segment which connects A, B, C, T with the center of the circle, respectively.

$$\sin^2\theta_{12} = \frac{((r_B\cos\theta_B - r_T\cos\theta_T)(r_C\sin\theta_C - r_T\sin\theta_T) - (r_B\sin\theta_B - r_T\sin\theta_T)(r_C\cos\theta_C - r_T\cos\theta_T))^2}{(r_B^2 + r_T^2 - 2r_B r_T\cos(\theta_B - \theta_T))(r_C^2 + r_T^2 - 2r_C r_T\cos(\theta_C - \theta_T))} \tag{3.28}$$

$$\sin^2\theta_{23} = \frac{((r_B\cos\theta_B - r_T\cos\theta_T)(-r_T\sin\theta_T) - (r_B\sin\theta_B - r_T\sin\theta_T)(r_A - r_T\cos\theta_T))^2}{(r_B^2 + r_T^2 - 2r_B r_T\cos(\theta_B - \theta_T))(r_A^2 + r_T^2 - 2r_A r_T\cos(\theta_A - \theta_T))} \tag{3.29}$$

$$\sin^2\theta_{13} = \frac{((r_A\cos\theta_A - r_T\cos\theta_T)(r_C\sin\theta_C - r_T\sin\theta_T) - (r_A\sin\theta_A - r_T\sin\theta_T)(r_C\cos\theta_C - r_T\cos\theta_T))^2}{(r_A^2 + r_T^2 - 2r_A r_T\cos(\theta_A - \theta_T))(r_C^2 + r_T^2 - 2r_C r_T\cos(\theta_C - \theta_T))} \tag{3.30}$$

In square and hexagonal region, the parameters in (3.6) are

$$\sin^2\theta_{12} = \frac{[(x_B - x_T)(y_C - y_T) - (y_B - y_T)(x_C - x_T)]^2}{[(x_B - x_T)^2 + (y_B - y_T)^2][(x_C - x_T)^2 + (y_C - y_T)^2]}, \tag{3.31}$$

$$\sin^2\theta_{23} = \frac{[(x_B - x_T)(y_A - y_T) - (y_B - y_T)(x_A - x_T)]^2}{[(x_B - x_T)^2 + (y_B - y_T)^2][(x_A - x_T)^2 + (y_A - y_T)^2]} \tag{3.32}$$

and

$$\sin^2\theta_{13} = \frac{[(x_A - x_T)(y_C - y_T) - (y_A - y_T)(x_C - x_T)]^2}{[(x_A - x_T)^2 + (y_A - y_T)^2][(x_C - x_T)^2 + (y_C - y_T)^2]}. \tag{3.33}$$

Because we have three reference nodes with unknown location in this assumed scenario,

the optimum position information can be obtained by minimizing

$$(\hat{x}_A, \hat{y}_A, \hat{x}_B, \hat{y}_B, \hat{x}_C, \hat{y}_C) = \text{argmin}\, \overline{MMSE}. \tag{3.34}$$

All the implements above will be simulated at one time and we will get the results at the same time.

Until now, we provide three common designs in three different shapes of region. This not only proves that our scheme is flexible but also gives a guidance for starting to set a localization system and obtain the optimum reference nodes placement.

3.4 Simulation Results

In this section, we present the numerical optimization results for the three reference nodes positioning in different scenarios, based on the deployment region of the target node as following.

3.4.1 Circular Region

In Figure 3.2, the optimum deployment topologies are shown when the location of the reference nodes are unknown (Figure 3.2-(a)), one reference node is fixed at the center of the region (Figure 3.2-(b)), two reference nodes are fixed in the region (Figure 3.2-(c) and -(d)).

As shown in Figure 3.2-(a), assuming three reference nodes can be deployed anywhere in the circular region, the best structure is when the reference nodes have equiangular distances, i.e., equal to 120°, around the center of the region. Also, their distances to the center are equal, which is 0.901 times the radius of the region. Figure 3.2-(b) shows the optimum case when a reference node, i.e., one base station, is located at the center of the circular region and two other reference nodes, e.g., two access points or mobile users, cooperate with this base station for

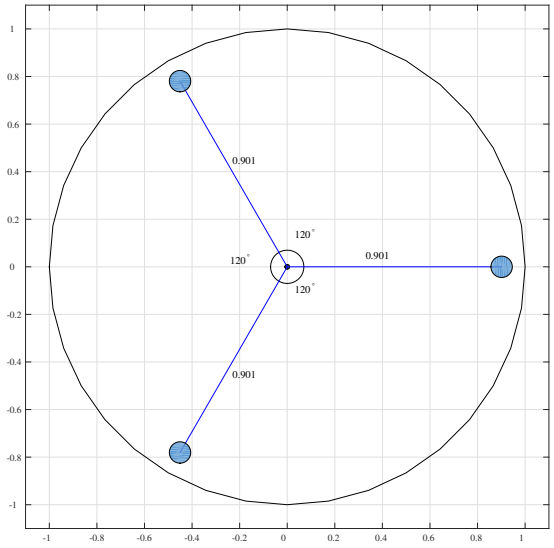

(a) three adjustable RNs

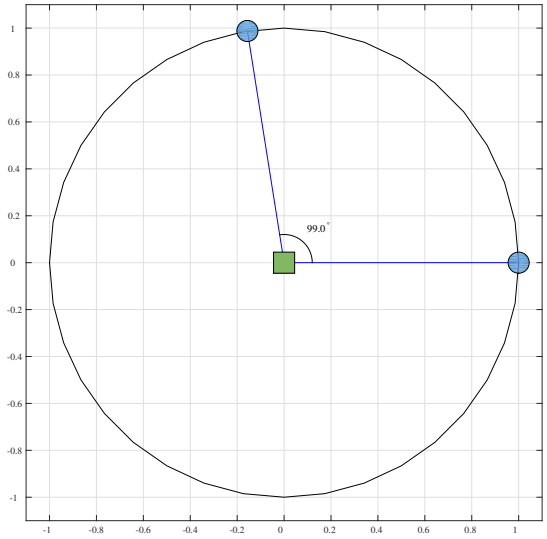

(b) two adjustable RNs

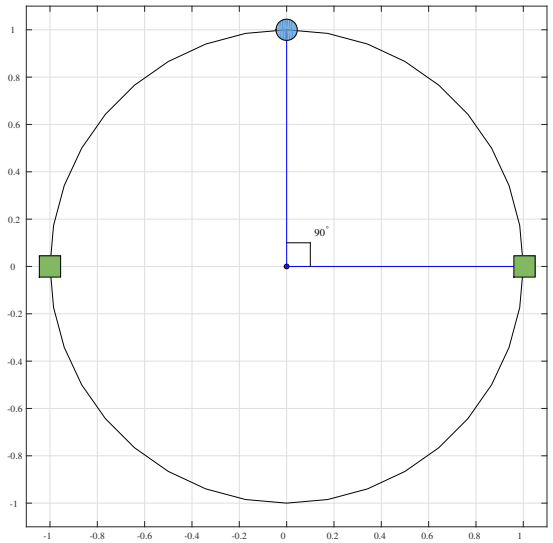

(c) one adjustable RN with fix RNs at the side

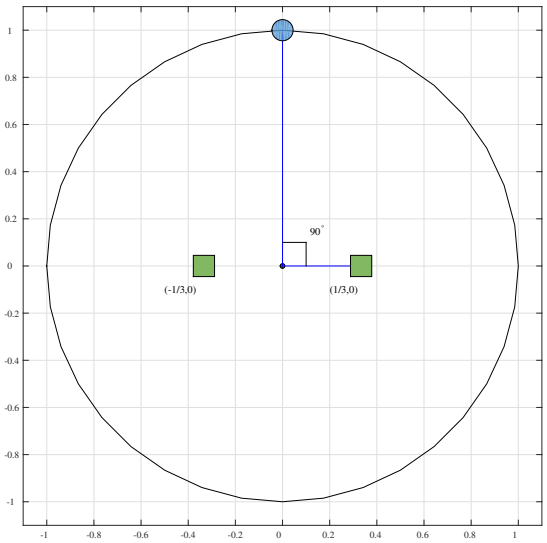

(d) one adjustable RN with fix RNs inside

Figure 3.2: Optimum RNs Placement Scheme Within Circular Region

localization. As the figure depicts, the optimum positions for the two reference nodes are on the circumference of the circle with angular distance 99.0° with respect to the center of the region. Figure 3.2-(c) and -(d) show the cases where two base stations are located on the diameter of the region symmetrically on two sides of the center, within and on the circumference of the circle, respectively. As seen, in both cases, the best position of the third reference node cooperating with the two base stations is on the intersection of the circumference of the circle and the perpendicular bisector of the base stations crossing line.

3.4.2 Hexagonal Region

Similar to the circular region case, the reference nodes placements shown in Figure 3.3 present three optimum localization conditions when no reference node is fixed (Figure 3.3-(a)), one reference node is fixed (Figure 3.3-(b)), and two reference nodes are fixed (Figure 3.3-(c) and -(d)).

For the first case where no reference node is fixed, the optimum locations of the three reference nodes are shown in Figure 3.3-(a). In this case, the reference nodes form an equilateral triangle within the hexagon which means they have equal angular distances 120° around the center of the region. In addition, the distances between the reference nodes and the center point are 0.804 times the side of the hexagonal region. In Figure 3.3-(b), a reference node as a base station is fixed at the center of hexagonal region and the other two reference nodes assist the base station to locate the target node in this region. From the result, we can find that the best positioning for the two reference nodes are at the boundary of the region with angular distance 105.0° with respect to the center point. In Figure 3.3-(c) and -(d), two base stations are locate on the central axis of the hexagonal region, symmetrically on two sides of the center point and separated one third of the diameter. The figures show that they have the same optimum reference node location which is at the middle of the region side which has equal distance to

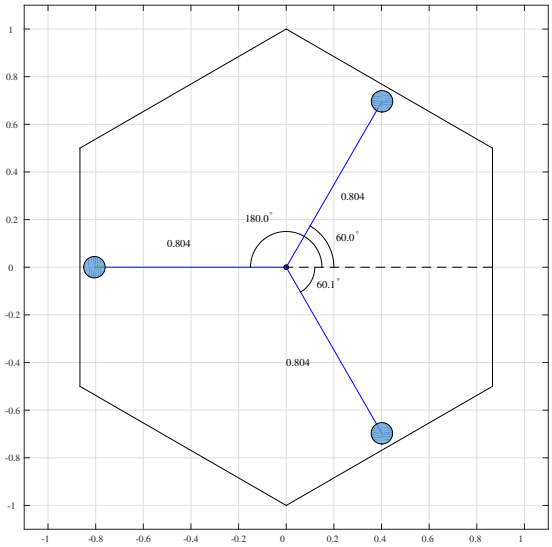

(a) three adjustable RNs

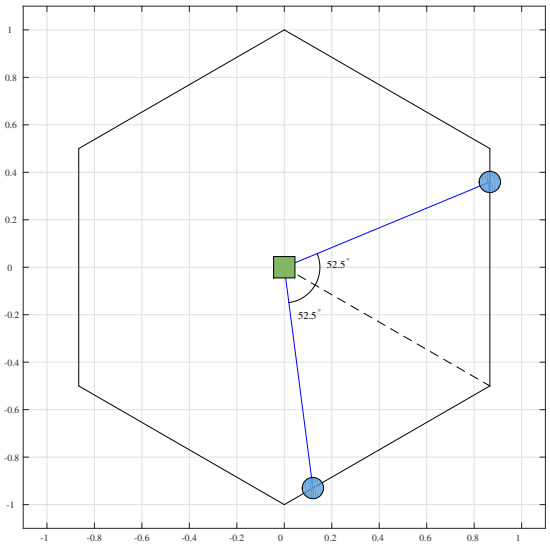

(b) two adjustable RNs

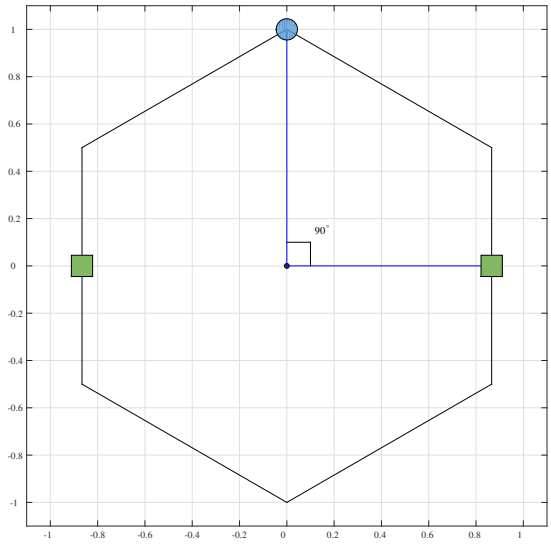

(c) one adjustable RN with fix RNs at the side

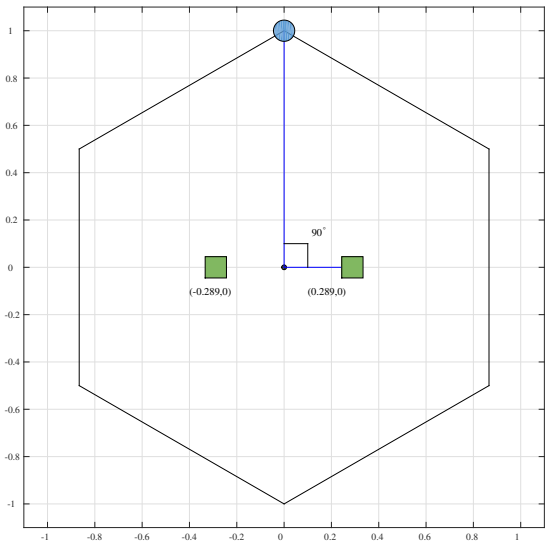

(d) one adjustable RN with fix RNs inside

Figure 3.3: Optimum RNs Placement Scheme Within Hexagonal Region

the base stations.

3.4.3 Square Region

In Figure 3.4, the optimum deployment topologies are shown for the square region, when the location of the three reference nodes are unknown (Figure 3.4-(a)), one reference node is fixed at the center of the region (Figure 3.4-(b)), and two reference nodes are fixed in the region (Figure 3.4-(c) and -(d)).

As depicted by Figure 3.4-(a), the optimum case when the the reference nodes can be located anywhere on the square region is similar to circular and hexagonal region cases, i.e., the angular separation between any two reference nodes is close to 120° and they maximally spread on the region. In addition, for the case where one reference node is fixed in the center of the region as a base station, the optimum location of the other two reference nodes are on the boundary of the square region with angular separation around 100°, which is close to what have been obtained for the circular and hexagonal regions. Furthermore, for the two base station case where two reference nodes are fixed in the region or on the boundary, as shown by Figure 3.4-(a) and Figure 3.4-(b), respectively, the optimum location of the third reference node is similar to those of the circular and hexagonal regions, i.e., on the boundary and on the perpendicular bisector of the base stations crossing line.

In fact, our proposed scheme can be used in any shape of region and the number of the base stations or the reference nodes with no prior localization can also be different. Besides, when our scheme is applied to the situation where there are 3 unknown base stations, it can in fact be used to establish a localization system in any wireless network.

Figure 3.5 shows the 50-iteration simulation results which compare the situations when we use the selected optimum reference nodes according to our proposed scheme with the reference

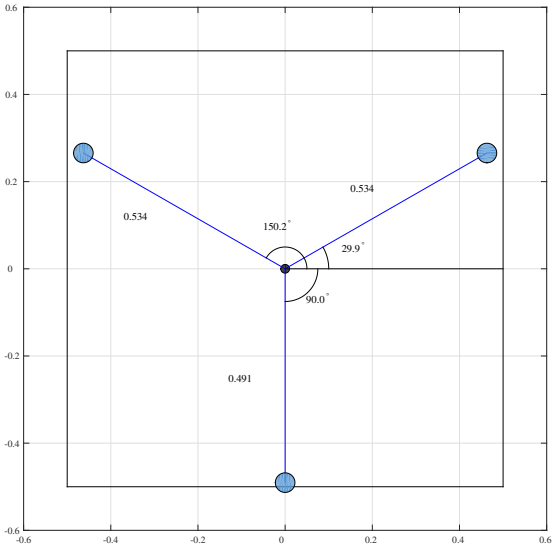

(a) three adjustable RNs

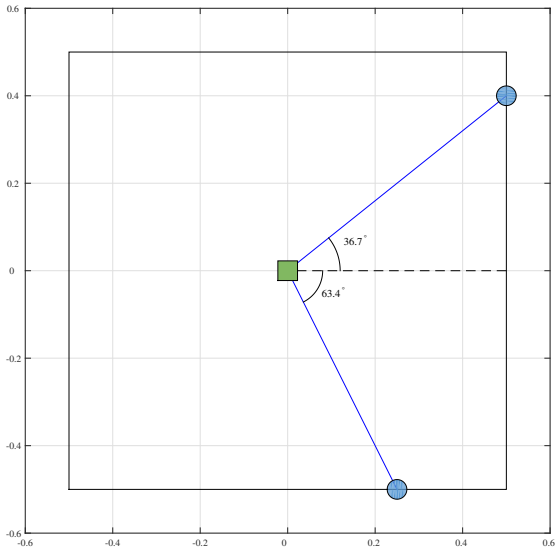

(b) two adjustable RNs

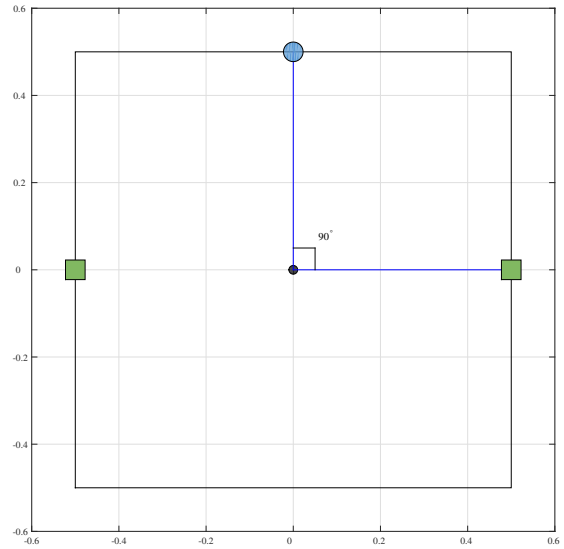

(c) one adjustable RN with fix RNs at the side

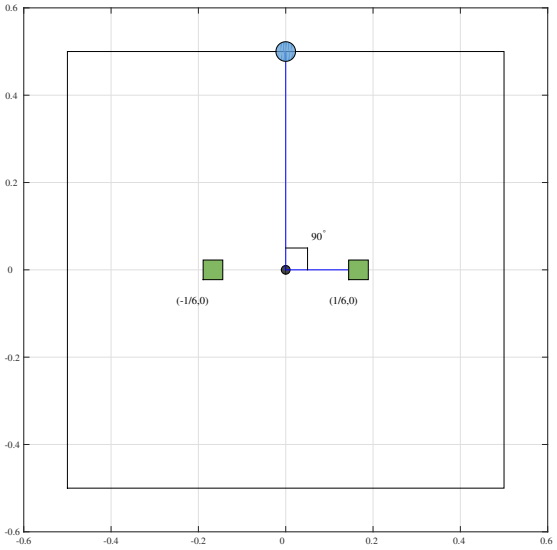

(d) one adjustable RN with fix RNs inside

Figure 3.4: Optimum RNs Placement Scheme Within Square Region

nodes randomly selected where we change location of one reference node among the optimum locations. In the simulation, we select four nodes which are in the center from four different quadrants as the target nodes and the distance between them and the central point is 0.5 in circular scenario. With iterations increasing, the variance of noise is increasing as well. As we can see in Figure 3.5, the accuracy can be increased by using our proposed reference nodes selection scheme.

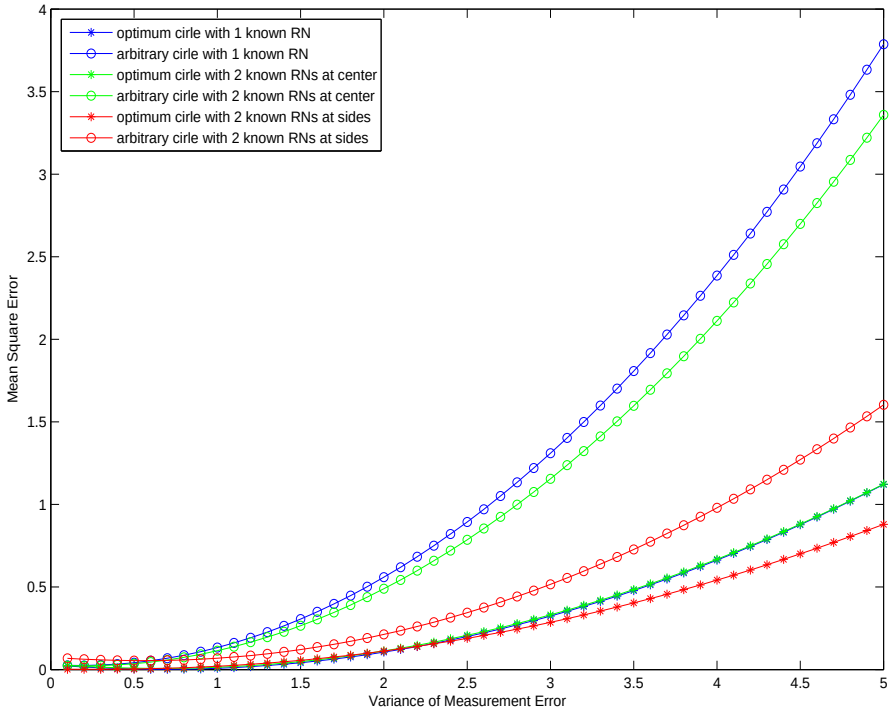

Figure 3.5: Mean Square Error Comparison Between Optimum RNs and Arbitrary RNs in Circular Region

3.5 Chapter Summary

In this chapter, we propose a general scheme in determining the optimum reference nodes deployment scheme. For illustration and demonstration for the flexibility of the scheme, we simulate our scheme in circular, hexagonal and square positioning regions. The proposed method can be applied in arbitrary region in realistic localization system. Besides, this scheme can

be practical when extending an existed localization system. As the average positioning performance was carried out, the best locationing performance of the reference node deployment could be determined as the lowest MSE average value within a certain area. It is shown from the simulation results that the proposed scheme improves the accuracy of location.

Chapter 4

Joint Localization Algorithm Combining Information from Accelerometer and Available Reference Nodes

In conventional wireless localization techniques, the performance is generally constrained by the number of reference nodes available in the communication range. Recently, alternative localization schemes have been proposed to utilize the internal sensors embedded in wireless devices to acquire additional useful location dependent parameters. The accelerometer based localization has attracted much attention because of the widely usage of accelerometer sensors in today's smart phones. However, the accumulated error from the sensors can decrease the localization accuracy significantly as time goes by. In this chapter, we propose a novel algorithm which combines the signal measurements from available reference nodes and the data output from accelerometer sensor to overcome the error accumulation. The simulation results shows that our proposed algorithm can achieve outstanding localization performance with only few reference nodes.

4.1 Introduction

With the growing demand for LBSs in recent years, location estimation has already become an essential enabling technology in many emerging wireless applications [51], such as health care [52], smart homes [53], social network [54], monitoring [55], tracking and navigation [56]. In cellular network, the Enhanced 911 (E-911) service is mandated by the Federal Communications Commission to locate the positions of mobile users who call the emergency number [57]. In Wireless Sensor Networks (WSNs), the geographical location information of the sensor nodes is essential for the sensed data to be useful [58]. As a result of these increasing demand for LBSs, accurate localization for a certain target has been highlighted.

The target location is generally estimated through some location dependent parameters measured from a set of reference nodes whose positions are known as priori in traditional wireless localization schemes. Therefore, the localization performance is constrained by the number of reference nodes available within the communication range of the target node. In addition, the usual localization methods which measure location dependent parameters, such as ToA [59], AoA [60] and RSS [61], are highly sensitive to the communication environment and the system calibration. The multipath effect and addictive noise are two major sources which degrade the localization accuracy in complex environment. In ToA and AoA based localization schemes, system calibration and synchronization also have significant impact on the localization performance. RSS based localization systems are more easy to implement as it does not require any additional hardware. The reference nodes in RSS based position system can provide relatively reliable localization information.

Due to the exponential growth of the smartphone market in recent years, alternative localization schemes have been proposed to utilize the internal sensors embedded in smartphones to obtain additional location dependent parameters and improve localization performance [62]. Most of today's smartphones are equipped with various built-in sensors, providing extremely

useful information which can not only be used in today's mobile applications for entertainment and user interaction purposes, but also in many emerging wireless applications. Accelerometer is one of the internal sensors which can output the accelerations from different directions of the device. In this way, the moving distance of a user can be calculated through the acceleration information for position estimation. However, the accuracy of localization based on accelerometer is highly sensitive to the sensor measurement error. In addition, the sensor error can be accumulated along with the time increase, which will degrade the localization performance significantly.

Considering the existing problems in above discussed localization schemes, we consider to combine two different types of location dependent parameters measured from available reference nodes and internal accelerometer sensor altogether in order to overcome the drawbacks and improve the localization performance. A noticeable work has been presented in [58], where the authors combine the accelerometer information with the RSS fingerprinting based on interval analysis. However, the RSS fingerprinting map generation is labor-intensive and time-consuming. In addition, the map needs to be updated when the environment in the localization system changes. In this paper, we propose a novel algorithm to combine the information from accelerometer and available reference nodes through weighted least square error (WLSE) of the two different types of information to minimize the localization error. As shown in our simulation results, by use of the proposed combined localization method, the error accumulation from the accelerometer can be eliminated with the help of very few reference nodes involved, and the localization accuracy can be improved significantly.

The rest of the paper are organized as follows: In Section II, we present the accelerometer based localization method and do experiment to show the error accumulation, while the combined algorithm is proposed in Section III. Simulation results are given in Section IV.

4.2 System Model

4.2.1 Accelerometer based localization

Accelerometer sensor is one of the most important features in smartphones. The data output from the accelerometer sensor in most of today's smartphones is according to the coordinate system as shown in Figure 4.1. The positive x axis points to the right of the screen, the positive y axis points to the up of the screen, and the positive z axis points towards the outside of the front face of the screen. The accelerometer measures the portable device's acceleration along three axes.

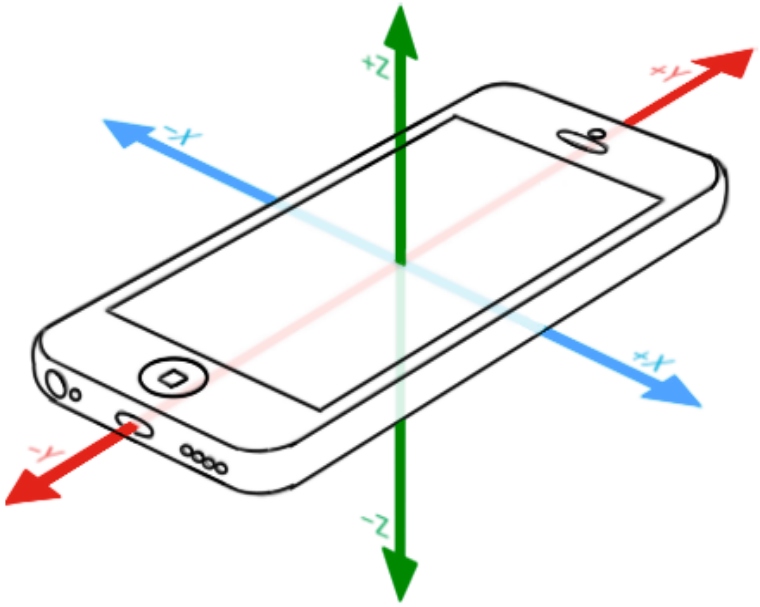

Figure 4.1: Coordinate system of data output from accelerometer in smartphones.

In accelerometer based localization scheme, the acceleration data along the three orthogonal axes obtained from the embedded accelerometer sensor is used to calculate the moving distance of the target device for localization purpose. Assume the target starts moving from time slot t_0, and the initial acceleration at t_0 is 0 m/s^2. Let $a(t)$ denote the acceleration at time

slot t, the moving velocity along the acceleration direction at time slot t can be obtained as

$$v(t) = \int_{t_0}^{t} a(x)dx. \tag{4.1}$$

Then the moving distance of the user at time slot t can be calculated by

$$d(t) = \int_{t_0}^{t} v(x)dx = \int_{t_0}^{t}\int_{t_0}^{y} a(x)dxdy. \tag{4.2}$$

In practical, the sampling data from the accelerometer sensor is in discrete time. Let $\triangle t$ denote the sampling period of the accelerometer sensor and assume the acceleration of the target remains unchanged during the very short sampling period, then the moving velocity along the acceleration direction at the nth sampling point can be expressed as

$$v(t_n) = \sum_{k=1}^{n} a(t_k)\triangle t, \tag{4.3}$$

where $t_k = t_0 + k\triangle t$ is the time slot of the kth sampling point. Alternatively, we can calculate the target moving velocity at current sampling time based on the velocity at previous sampling time, which can be expressed as

$$v(t_n) = v(t_{n-1}) + a(t_n)\triangle t, \tag{4.4}$$

where $a(t_n)$ is the acceleration during the sampling period ($\triangle t$) from t_{n-1} to t_n. Then the moving distance from time slot t_0 which is the starting point to time slot t_n can be calculated as

$$\begin{aligned} d(t_n) &= d(t_{n-1}) + \frac{1}{2}[v(t_{n-1}) + v(t_n)]\triangle t \\ &= d(t_{n-1}) + v(t_{n-1})\triangle t + \frac{1}{2}a(t_n)\triangle t^2. \end{aligned} \tag{4.5}$$

Let e_n denotes the error of the acceleration measurement data a_{t_n}, then the velocity at the nth

sampling point $v(t_n)$ in (4.4) becomes

$$\begin{aligned} v(t_n) &= v(t_{n-1}) + [a(t_n) + e_n]\triangle t \\ &= v(t_{n-1}) + a(t_n)\triangle t + e_n\triangle t. \end{aligned} \tag{4.6}$$

Therefore, the moving distance at the nth sampling point $d(t_n)$ in (4.5) can be calculated as

$$\begin{aligned} d(t_n) &= d(t_{n-1}) + \frac{1}{2}[v(t_{n-1}) + v(t_n)]\triangle t \\ &= d(t_{n-1}) + v(t_{n-1})\triangle t + \frac{1}{2}a(t_n)\triangle t^2 + \frac{1}{2}e_n\triangle t^2. \end{aligned} \tag{4.7}$$

As shown in (4.7), the error of distance calculation in the previous sampling time will be accumulated to the distance estimation in the current sampling time because of the accelerometer measurement error. Therefore, the measurement error will increase significantly when the sampling time gets longer.

4.2.2 Accelerometer and available reference node combined localization algorithm

In this section, we combine the location dependent parameters measured from available reference nodes and accelerometer sensor altogether through Weighted Least Square Error (WLSE). With involving the available reference nodes, the combined localization algorithm will be able to eliminate the error accumulation from the accelerometer while overcoming the limitation of conventional localization schemes.

Consider a user holding a device equipped with both accelerometer sensor and wireless communication module which enables the device to measure the signal strength from available reference nodes in its communication range, the location dependent parameters obtained from the sensor and the received wireless signals can be combined together to improve the localiza-

tion performance. Assume there are N reference nodes available within the user's communication range, the distance measurement error between the target and the ith reference node can be expressed as

$$e_{r,i}(x, y) = d_{m,i}(m_i) - d_{r,i}(x, y), \tag{4.8}$$

where (x, y) is the true position of the user, m_i is the measured location related parameter from the ith reference node, and $d_{m,i}(m_i)$, $d_{r,i}(x, y)$ are the measured distance and the real distance between the target and the ith reference node, respectively. Let (x_i, y_i) denotes the position of the ith reference node, the real distance can be calculated as

$$d_{r,i}(x, y) = \sqrt{(x - x_i)^2 + (y - y_i)^2}. \tag{4.9}$$

The measured distance $d_{m,i}(x, y)$ can be measured through conventional localization methods , such as RSS and ToA, based on corresponding signal propagation models.

In RSS-based localization, the relationship between the received signal strength from the ith reference node and the distance can be modeled as

$$d_{m,i}(rss_i) = d_0 \cdot 10^{(P_0 - rss_i)/10\alpha}, \tag{4.10}$$

where P_0 is the signal power in decibel at the reference distance d_0 away from the transmitter, rss_i is the measured signal strength from the ith reference node, and α is the path loss exponent which is an environment dependent parameter. The reference distance d_0 is typically set to be $1m$.

In ToA-based localization, the measured time of arrival is related to the distance between the target and the ith reference node by

$$d_{m,i}(t_i) = c \cdot t_i, \tag{4.11}$$

where c is the parameter of signal propagation speed, and t_i is the measured signal propagation time from the ith reference node.

In combined localization algorithm, we minimize the weighted square error of the distance estimation from reference nodes and accelerometer in order to eliminate the error accumulation and improve the localization accuracy. Assume (x_{n-1}, y_{n-1}) is the estimated target location at the $(n-1)$th sampling point, we first calculate the moving distances along x and y axis at the nth sampling point by

$$\begin{cases} x'_n = x_{n-1} + \frac{1}{2}(2v_{x,n-1} + a_{x,n}t)t, \\ y'_n = y_{n-1} + \frac{1}{2}(2v_{y,n-1} + a_{y,n}t)t, \end{cases} \tag{4.12}$$

where $(v_{x,n-1}, v_{y,n-1})$ is the target moving velocity at the $(n-1)$th sampling point, and t is the time duration between the previous and the current sampling point. Let $(v_{x,0}, v_{y,0})$ denote the initial velocity, then (4.12) can be expressed as

$$\begin{cases} x'_n = x_{n-1} + \frac{1}{2}(2v_{x,0} + 2\sum_{k=1}^{n-1} a_{x,k}t + a_{x,n}t)t, \\ y'_n = y_{n-1} + \frac{1}{2}(2v_{y,0} + 2\sum_{k=1}^{n-1} a_{y,k}t + a_{y,n}t)t. \end{cases} \tag{4.13}$$

Let $\Delta a_{k,x}$ and $\Delta a_{k,y}$ denote the accelerometer measurement error at the kth sampling point along x and y axis, respectively, then the accumulated error at the nth sampling point can be calculated as

$$\begin{cases} e_{n,x} = \sum_{k=1}^{n-1} \Delta a_{k,x}t^2 + \frac{1}{2}\Delta a_{n,x}t^2, \\ e_{n,y} = \sum_{k=1}^{n-1} \Delta a_{k,y}t^2 + \frac{1}{2}\Delta a_{n,y}t^2. \end{cases} \tag{4.14}$$

In this way we can combine the distance estimation from accelerometer and reference nodes

together, based on WLSE algorithm. The combined weighted square error can be expressed as

$$S(x_n, y_n) = \sum_{i=1}^{N} w_{r,i} \cdot e_{r,i}^2(x_n, y_n) + w_a \cdot (x_n - x'_n)^2 + w_a \cdot (y_n - y'_n)^2, \tag{4.15}$$

where $e_{r,i}$ is the distance measurement error from the ith reference node in (4.9), $w_{r,i}$ and w_a are the weights from the ith reference node and from the accelerometer at nth sampling point, respectively. We assign the weights to the square errors based on the corresponding variances. The variance of distance estimation error from the ith reference node can be obtained as a known parameter according to the signal propagation model, denoted as $\sigma_{r,i}^2$, while the variance of the random error from the accelerometer can be also known as a priori, denoted as σ_a^2.

4.2.3 Weighted assignments for accelerometer and reference nodes

For most data sets, appropriate weights specifications are recommended since they output better performance. Generally, the best weight of a data is reciprocal of data point's variance. The weighting assignments of localization information from accelerometer sensor and reference nodes we use here is a very common scheme whose weights are proportional to the inverse of the variance values as presented below:

$$w_1 : w_2 : ... : w_n = \frac{1}{\sigma_1^2} : \frac{1}{\sigma_2^2} : ... : \frac{1}{\sigma_n^2}, \tag{4.16}$$

where $w_1, w_2, ..., w_n$ indicate the weight of every data in a data set and $\sigma_1, \sigma_2, ..., \sigma_n$ are corresponding standard deviations. Based on the calculated total error from accelerometer sensor and avaliable reference nodes in (4.15) and the weight scheme presented in (4.16), we assign

the weights to localization information collected from reference nodes and accelerometer by

$$\begin{cases} w_{r,i} = \dfrac{\frac{1}{\sigma_{r,i}^2}}{\sum_{i=1}^{N} \frac{1}{\sigma_{r,i}^2} + \frac{2}{\sigma_d^2}}, \\ w_a = \dfrac{\frac{1}{n\sigma_d^2}}{\sum_{i=1}^{N} \frac{1}{\sigma_{r,i}^2} + \frac{2}{\sigma_d^2}}, \end{cases} \tag{4.17}$$

where $\sigma_d^2 = (\frac{1}{2}\sigma_a t^2)^2$. Therefore, the location estimation result at the nth sampling point using combined localization scheme can be expressed as

$$(x_n, y_n) = \arg\min_{x_n, y_n} S(x_n, y_n). \tag{4.18}$$

By using the combined localization scheme, we can minimize the measurement error accumulated from accelerometer with the help of a few reference nodes in its communication range. Moreover, the localization performance can become more stable in harsh environment since the data output from internal accelerometer sensor is not affected by the environment change.

4.3 Simulation Results

The simulation process includes two parts. The first step is to collect the real data from the smartphone which will present the existence of accelerometer measurement error. Then the performance of the situations only use acceleration information and combined algorithm utilizing both sensor data and anchor node knowledge are compared.

4.3.1 IOS based platform

To show the error accumulation of the accelerometer based localization method, we do experiment on iOS smartphone (Iphone 5c). An iOS application has been developed using the newest Apple's language called Swift. Apple developer used to use Objective-C code to design the application, however, Objective-C is difficult for new developers who are not familiar with C. As a result of it, other language like Java, Javascript and Python are becoming more popular and lots of developer write codes using these programming languages. Since less developers use Objective-C, the applications for iOS and OS X are increasing slowly. Due to all the reasons above, Apple published a new programming language called Swift for developing iOS and OS X applications. Swift continuously support Objective-C code but is faster than it. Besides, Swift has all the features other modern programming languages have and is extremely safe to use since it eliminate lots classes of unsafe codes. We use Swift also because it turns out to be easy to learn and use.

We use Swift to develop an application called "acceleration measurement" based on iOS 9.2[1] to utilize the linear accelerometer sensor embedded in the smartphone which can output the acceleration data excluding the force of gravity.

4.3.2 Smartphone-based measurement

After running acceleration measurement application, we get the real sensor data as presented in Figure 4.3. It shows the measured acceleration data along x and y axis when the phone is put stationary on the table. We can see the existing non-zero acceleration error, which is caused by the sensor measurement error.

Then we calculate the moving distance along x and y axis based on the measured acceler-

[1] Available in App store: `https://appsto.re/ca/VW9vbb.i`.

Figure 4.2: Interface of running Acceleration Measurement application.

ation error by use of (4.4) and (4.5). As shown in Figure 4.4, the sensor measurement error is accumulated on the distance estimation when time increases, which will degrade the localization accuracy significantly.

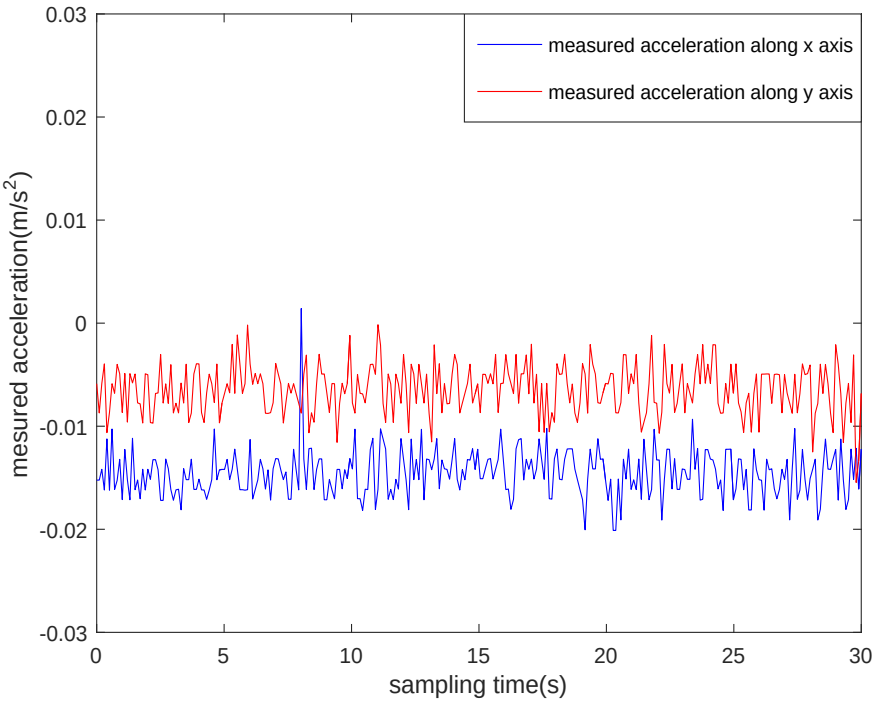

Figure 4.3: Measured acceleration along x and y axis from linear accelerometer when the phone is put stationary on the table.

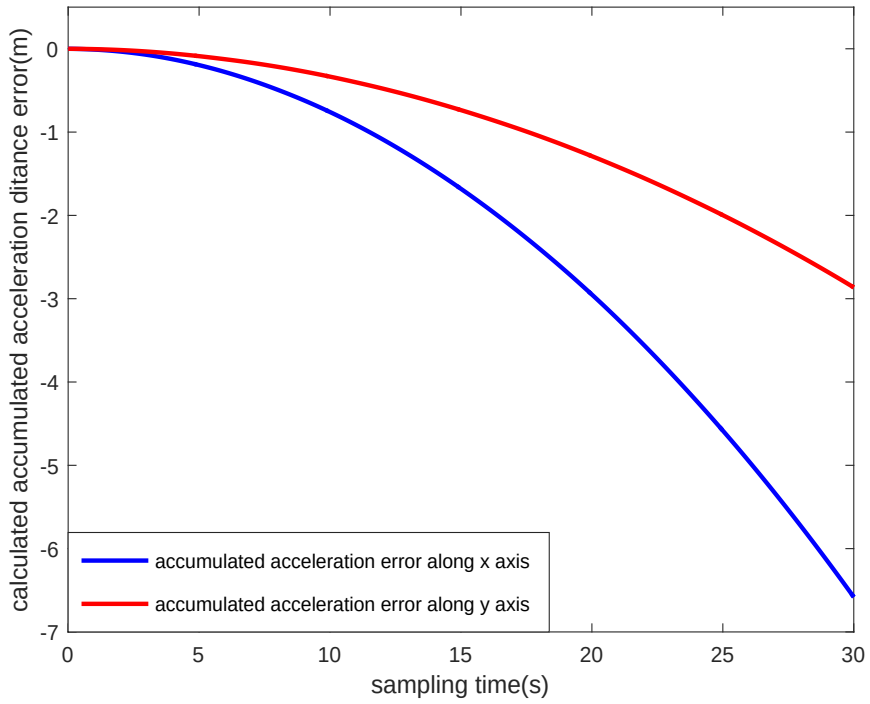

Figure 4.4: Moving distance caused by sensor measurement error.

4.3.3 User trajectory simulation

In the simulations, we first generate a random target moving trajectory and localize the target by using only accelerometer data. We set a random acceleration between each two sampling point from $-2m/s^2$ to $2m/s^2$, and set the sampling period to $0.05s$. The standard deviation of error from accelerometer is set to $0.2m/s^2$. Figure 4.5 shows the generated real target trajectory and the estimated trajectory using accelerometer with 1000 sampling points. From the trajectory in Figure 4.5 we can simply observe that the error is becoming larger because of the accumulated accelerometer error which is undesirable in localization system.

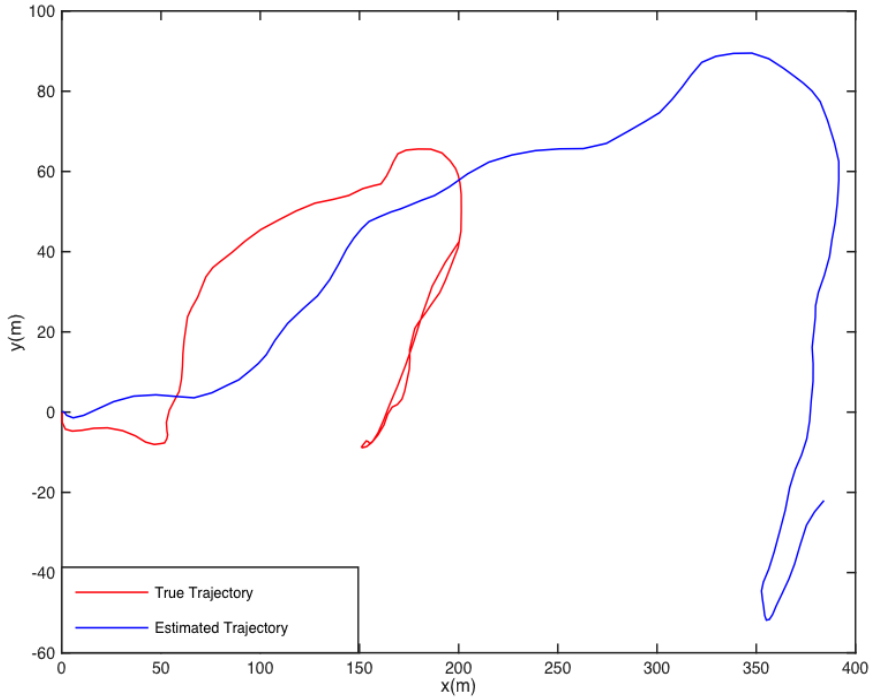

Figure 4.5: Real trajectory and estimated trajectory using accelerometer.

In order to compare the localization results between with and without information from reference nodes, we set one reference node at the starting point of the moving target which is the black point at $(0, 0)$ in Figure 4.6.

To show and compare the multiple reference nodes combined scheme, we move the target in another scenario whose trajectory is fixed and anticlockwise on a circle with radius of $10m$,

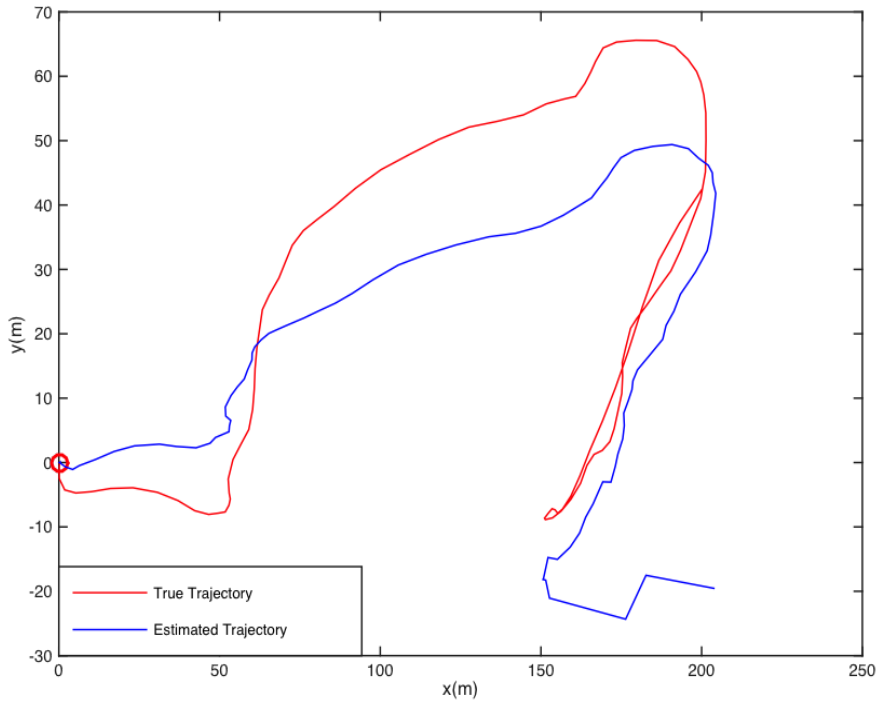

Figure 4.6: Real trajectory and estimated trajectory using accelerometer and avialible reference node.

starting from coordinate $(10, 0)$ and ending at the same position. The velocity of the target is set to $0.2\pi\ m/s$, and we set the sampling time to $1s$. The standard deviation of error from accelerometer and the distance measurement based on reference nodes are set to $0.2m/s^2$ and $0.5m$ respectively. The localization results of the target using only acceleration information is shown in Figure 4.7. With the time increasing, we can see the error is accumulated and the difference between the localization result and the true target location can become very large.

Then, we combine data from reference nodes and acceleration information to minimize the entire error. We deploy the reference nodes inside the circle. In Figure 4.8 (a) and (b), we set the amount of reference nodes from 2 to 3 which gives us desirable results. The simulation results also reveal that with the help of more reference nodes, the error become smaller.

In Figure 4.9, it compares the localization error between the scheme which is only using accelerometer and the solution we provide which includes the information from reference nodes.

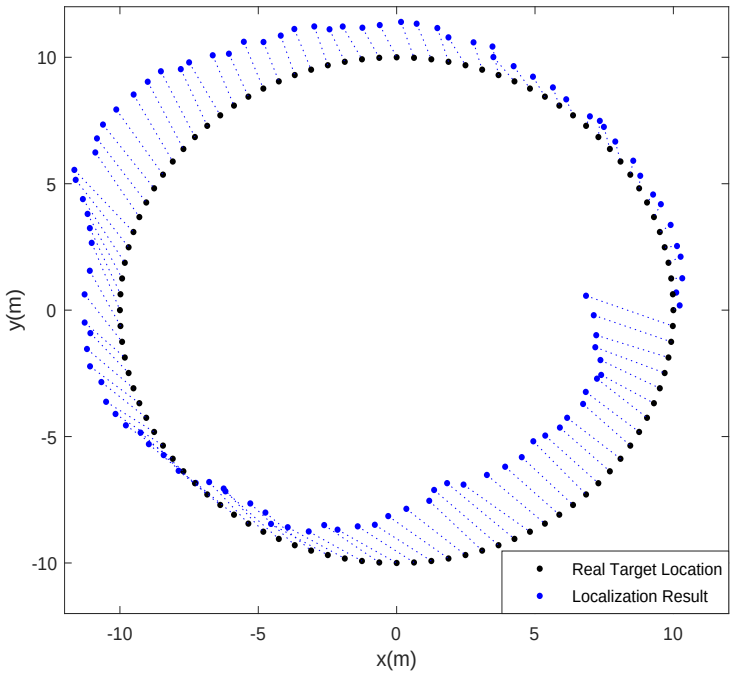

Figure 4.7: Real and estimated locations with only accelerometer.

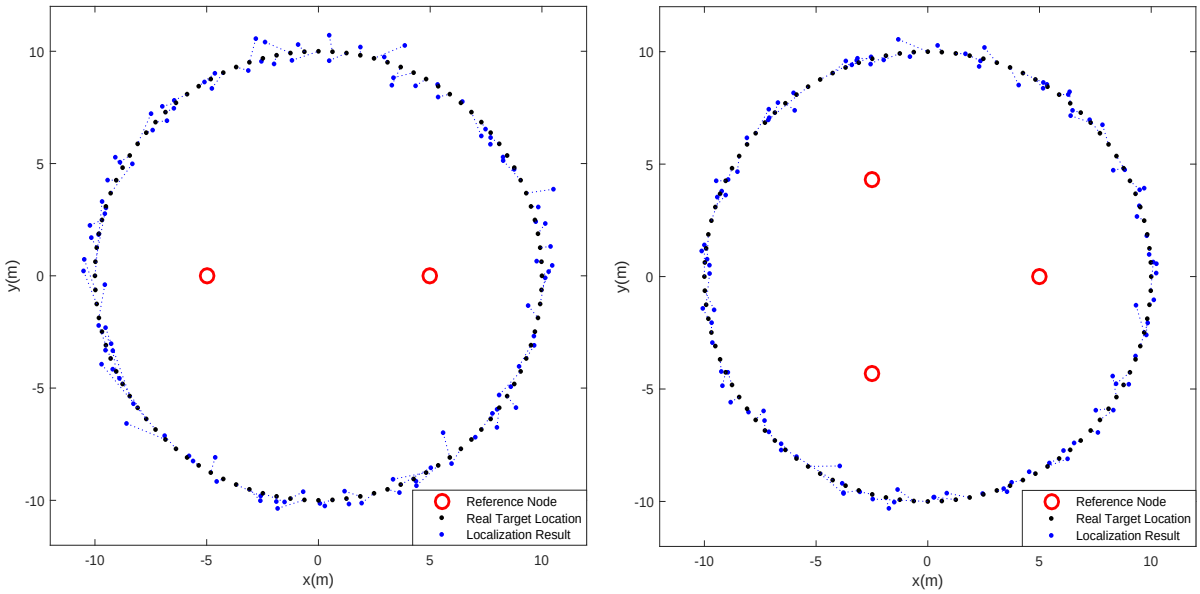

Figure 4.8: Real and estimated locations with both accelerometer and reference nodes.

We increase the sampling point from 100 to 500 in order to have a more clear view in this simulation result. From the result we can simply conclude that the localization error decrease a lot when we use the combined algorithm which will definitely give better positioning output.

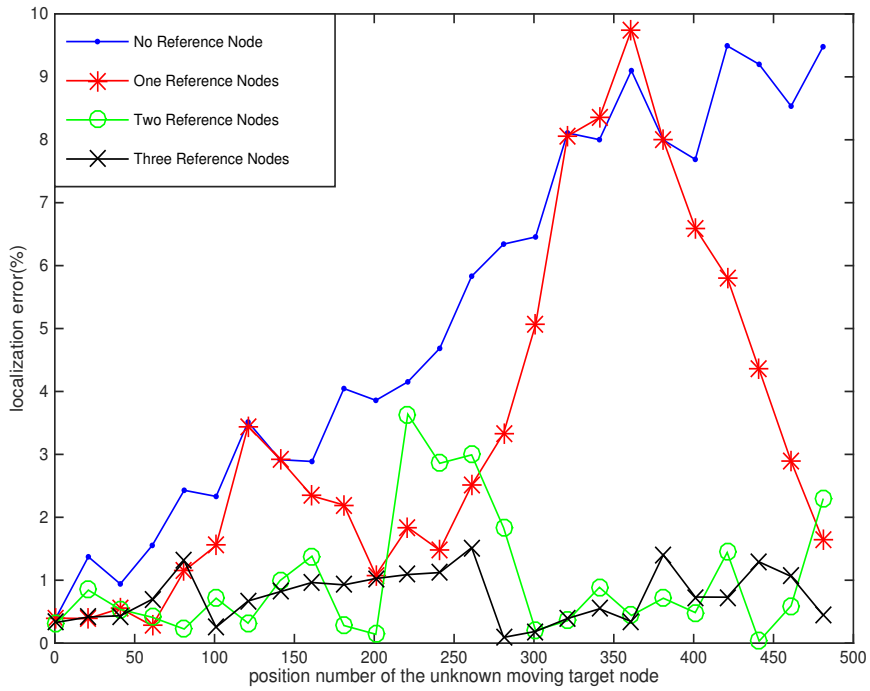

Figure 4.9: Localization error comparison between with and without reference nodes.

4.4 Chapter Conclusion

In this chapter, we analyze the error from accelerometer and reference node to combine these two different types of localization error together in order to eliminate the entire error. The proposed novel algorithm can be applied to any situation where we use devices equipped with accelerometer. This algorithm minimize the measurement error from the reference nodes as well as the internal error form the accelerometer which is accumulated as time goes by. As the simulation results carried out, we can obtain that our solution achieve good localization performance.

Chapter 5

Improving Log-distance Path Loss Localization Model by Utilizing Frequency Diversity

As the need for portable devices is increasing quickly these years, the ability to determine the position of portable device is a key feature. Among all the techniques which can be used to measure the distance between two nodes, RSSI based localization method is a simple and cost efficient technique as it uses the radio chip inside the portable devices itself (Bluetooth, Wi-Fi). Path loss is an essential characteristic of signal propagation, which can be used to predict the expected received power. A noticeable aspect of path loss is that it is frequency dependent which causes variations typically within a few MHz. As a result of it, RSSI can be influenced heavily due to external interference such as the carrier frequency and causes high variability in RSSI measurement. In this chapter we analyze the impact of different frequency on path loss and utilize the frequency diversity to get better localization results. We also present experimental results which is carried out on Software Defined Radio (SDR).

5.1 Introduction

Localization is a process of estimating the locations of specific targets by some detectable environmental parameters. GPS technology is popular in outdoor localization as it is available to anything with a GPS receiver to locate itself. Since signal from the GPS is in relatively high frequency, the microwave signals from GPS are scattered and attenuated by walls and other obstacles. These large attenuation indicates that the GPS is not suitable to be used in indoor localization. Thus, the indoor localization field remains a large research field and lots of techniques have been proposed to solve this urgent problem.

In indoor localization, the target indicates the object to be located while the anchor indicates the transceivers at a known fixed position. Five proposed localization technologies for indoor environment are radio frequency including ToA and RSSI techniques, photonic methods like image processing, sonic waves, mechanical measurements including inertial sensor data and other measured technologies such as magnetics and atmospheric pressure [63].

During the recent decades, people have proposed a large variety of RSSI-based localization methods to estimate the distance between the target and the anchors. RSSI-based localization technology is a simple method to estimate the location of the target as this technique only need hardware components to measure the signal strength. The authors present a simple method in [64] where the target only request for a few location information from anchors within its communication rage called centroid localization. The fundamental idea of centroid localization is to consider the centroid point of the surrounding anchors as the estimated target and it is first presented in [65]. However, this method can exist large error on the signal strength measurements due to a few factors such as obstacles, antenna characteristics and interferences. To improve this algorithm, a weighted centroid localization is presented in [66] which is relying on the distance of the anchors to the target. When the anchor is further, the weight is assigned small in this algorithm since the shadowing and other interferences can occupy large portion

of the fading when the anchor is further. Because of the variance caused by the enviroment, the accuracy of path loss measurements can vary in a relatively large scale which is vital in the localization system. Thus, a diversity concept come up to be a solution to decrease the fluctuation. The diversity of frequency is one of them which can be utilized to narrow the fluctuation of shadowing effect.

As the signal fading characteristics are depending on frequency and other interferences from the environment, the accuracy could be improved by adding multiple frequency estimations. In [67], the authors present a method for the target to make use of information from multiple channels using the weighted centroid localization algorithm. The target has two antennas receiving two different frequencies on the board of the platform while the bacons have four antennas to transmit and receive the signal at these frequencies seperately. To employ this frequency diversity method, an adaptive weighted centroid localization algorithm is proposed to improve the accuracy. The author later on introduces a modified scheme in [68] where a sensor data fusion is added. A Kalman filter is used to estimate the error from the inertial measurement such as acceleration and angular rate in this improved algorithm.

5.2 System Model

In RSSI method, the fingerprinting technique uses radio map database to localize a target but it is expensive and time consuming as its offline stage has to be done manually and needs to update frequently. However, the propagation model can help to give another solution where the emitted signal's intensity decreases while distance increases[69]. It is commonly considered to be implemented under trilateration scenario.

5.2.1 Trilateration

Trilateration is one of the most commonly used localization scheme[70][71][72]. As shown in Figure 5.1, T1, T2 and T3 are transmitters (usually WiFi access points or signal stations), which can send multiple carrier frequencies of carrier waves. R is the receiver (usually a mobile device), which has measurable distances from transmitters.

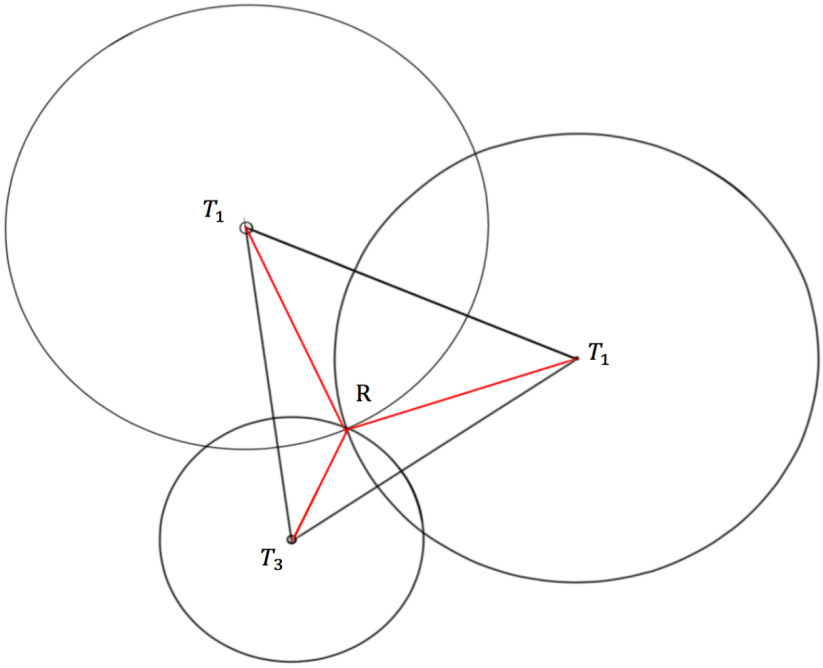

Figure 5.1: Trilateration, a general localization scheme.

If we set the position of R, T_1, T_2 and T_3 to (x_0, y_0), (x_1, y_1), (x_2, y_2), (x_3, y_3) separately, according to Pythagorean theorem, we can get

$$(x_1 - x_0)^2 + (y_1 - y_0)^2 = d_1^2 \tag{5.1}$$

$$(x_2 - x_0)^2 + (y_2 - y_0)^2 = d_2^2 \tag{5.2}$$

$$(x_3 - x_0)^2 + (y_3 - y_0)^2 = d_3^2 \tag{5.3}$$

Trilateration scheme demands prior knowledge of transmitters' positions and distances between them and the receiver, which can be measured by RSS, ToA and AoA techniques. However, the trilateration has only one internal check, which may cause large error. To reinforce the trilateration, we modified observational technique to offer larger number of measurements in order to narrow the localization error.

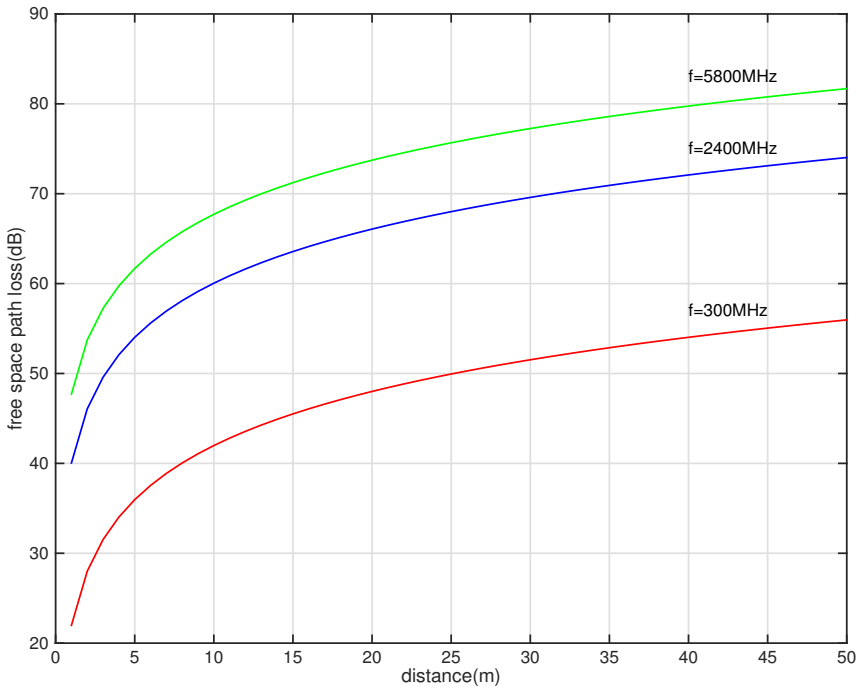

Figure 5.2: Path loss under different signal frequency.

5.2.2 System model

Frequency based path loss model

According to the log-distance path loss model based on the frequency, we can get

$$PL = 10nlog_{10}(d) + 20log_{10}(f) + 20log_{10}(\frac{4\pi}{c}) - G_t - G_r, \tag{5.4}$$

where PL is the path loss at distance d from the transmitter to the receiver, n is the path loss exponent, f is the signal frequency in, c is the speed of light. G_t and G_r is the antenna gain of transmitter and receiver separately. Usually when frequency changes, the path loss exponent and path loss will change. If we set the scenario to free space, we can have different path loss at different frequency as shown in Figure 5.2.

As shown in Figure 5.3, in reality, we usually only have prior knowledge to the positions of T_1, T_2 and T_3 which can be used to get the distances r_{12}, r_{23} and r_{13} between them. In this case, we can get the angular information as follows

$$cos\angle T_1T_2R = \frac{d_1^2 - r_{12}^2 - d_2^2}{2r_{12}d_2}, \tag{5.5}$$

$$cos\angle RT_2T_3 = \frac{d_3^2 - r_{23}^2 - d_2^2}{2r_{23}d_2}, \tag{5.6}$$

$$\angle T_1T_2R + \angle RT_2T_3 = \angle T_1T_2T_3, \tag{5.7}$$

where d_1, d_2 and d_3 denote the distances between the transmitters and the target separately.

Integrated the above equations with the frequency based propagation models at T_1, T_2 and T_3:

$$PL_1 = 10nlog_{10}(d_1) + 20log_{10}f + 20log_{10}(\frac{4\pi}{c}) - G_t - G_r, \tag{5.8}$$

$$PL_2 = 10nlog_{10}(d_2) + 20log_{10}f + 20log_{10}(\frac{4\pi}{c}) - G_t - G_r, \tag{5.9}$$

$$PL_3 = 10nlog_{10}(d_3) + 20log_{10}f + 20log_{10}(\frac{4\pi}{c}) - G_t - G_r, \tag{5.10}$$

where the path loss from the transmitters to the receivers PL_1, PL_2, PL_3 can be measured by the wireless signal module and the signal frequency f, G_t, G_r is a prior knowledge to us, the distances can be derived for the localization of the target. Also, different frequencies give out different localization estimations which can help narrowing the error.

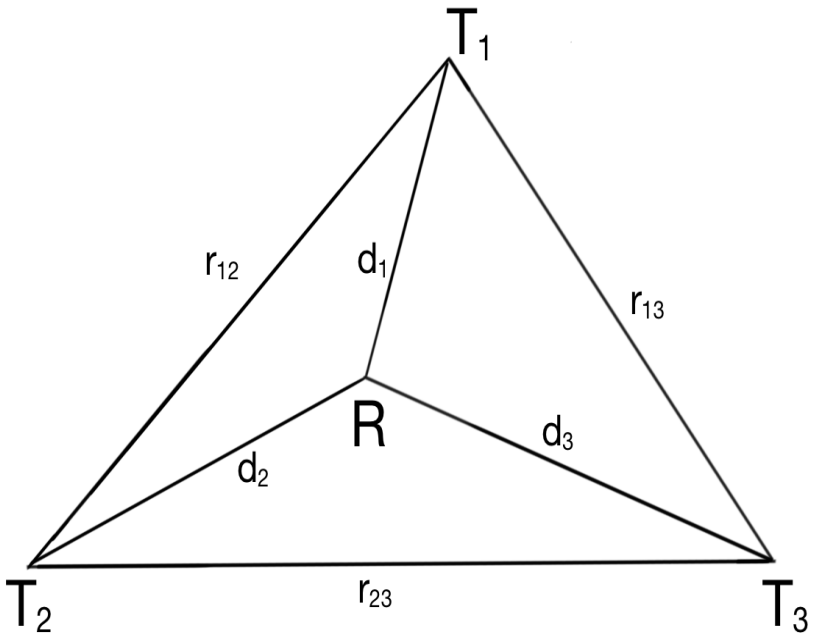

Figure 5.3: Illustration of frequency joint localization scheme.

Weighted algorithm

In the frequency diversity localization algorithm, there are multiple measurements estimating the position of the target. However, during the implementation, signal strength measurements experience fluctuation due to shadowing and fading caused by surrounding objectives.

The localization error $e(x, y)$ is defined as distance between the exact location $T(x, y)$ and the estimated location $T'(x', y')$ which can be presented as

$$e(x, y) = \sqrt{(x' - x)^2 + (y' - y)^2}. \tag{5.11}$$

If we simply take the average of the estimated locations from different frequencies, the

estimated position of the target is

$$T'(x', y') = \frac{1}{N} \sum_{i=1}^{N} T_i(x, y). \tag{5.12}$$

While this method only provides the final result by averaging the coordinates estimated by different frequencies, weighted based localization uses weights to improve the localization performance. Expressing the parameter N as adding all the ones, the Equation 5.12 can be expanded to

$$T'(x', y') = \frac{1}{\sum_{i=1}^{N} 1} \sum_{i=1}^{N} 1 \cdot T_i(x, y). \tag{5.13}$$

Since multiple frequencies are utilized in order to minimize the localization error, we will get several sets of measurements where we proposed a weighted scheme.

$$T(x, y) = \frac{\sum_{i=1}^{N} w_i \cdot T_i(x, y)}{\sum_{i=1}^{N} w_i}, \tag{5.14}$$

where $T_i(x, y)$ indicates the target location estimation by different frequencies, w_i is the corresponding weights at different frequencies.

Assume the path loss measurements at time t_0 is PL_0, however, due to the shadowing effect and other environment noise, the path loss fluctuates to PL_t at time t. Thus, with the same frequency, there exists a change of the path loss measurement ΔPL. As a result of it, the weight is equivalent to the function $1/\Delta PL$. The more fluctuation the signal is, the less weight is assigned to the localization information with the corresponding frequency. The weight is dependent on the deviation of the path loss:

$$w = \frac{1}{(\Delta PL)^g}, \tag{5.15}$$

where g is the degree parameter.

The degree parameter g here is to make sure that the signal which fluctuated a lot is still making affect on the localization estimation. When g is very high, the approximated position only receives the information from the most steady frequency signal which may increase the error $e(x, y)$. Thus, there exists a optimal g when the localization error $e(x, y)$ is minimum.

To define the parameter g, we collect the localization estimation results when frequency fluctuation varies. Firstly, we set the degree g from 0 to 8 as shown in Figure 5.4. The simple averaging scheme is the red line when g is equal to 0. From the simulation results we find that when g is between 1 and 2, the position determination error is relatively low. Thus, for the second step, we do the simulation while degree g is set from 1 to 2.1 as shown in Figure 5.5.

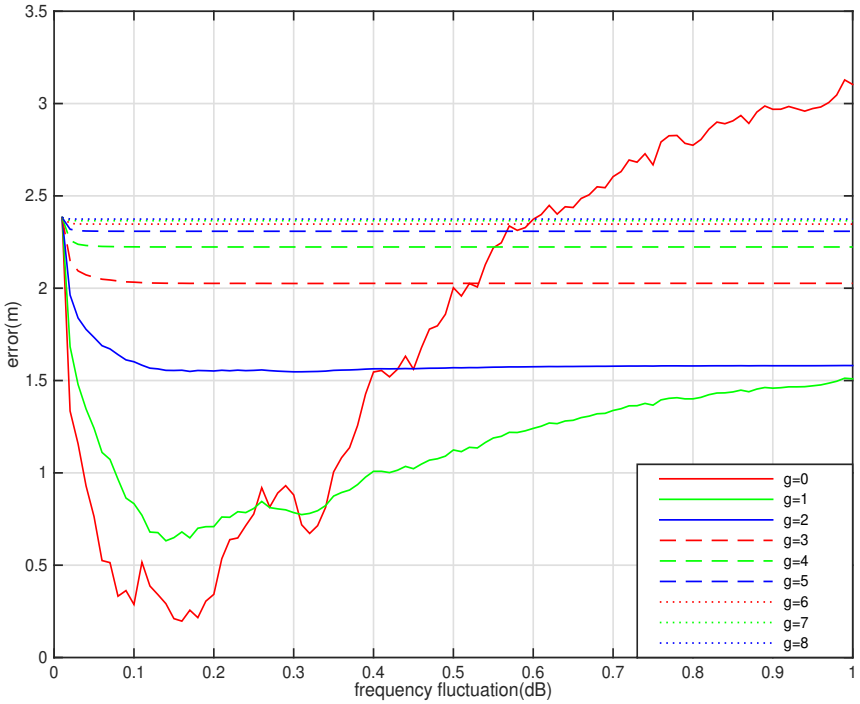

Figure 5.4: Localization error versus path loss fluctuation with different weight function while g is from 0 to 8.

According to the result presented in Figure 5.5, there are several minimum localization error depending on the frequency fluctuation range. It suggests put the degree to 1.5 if the

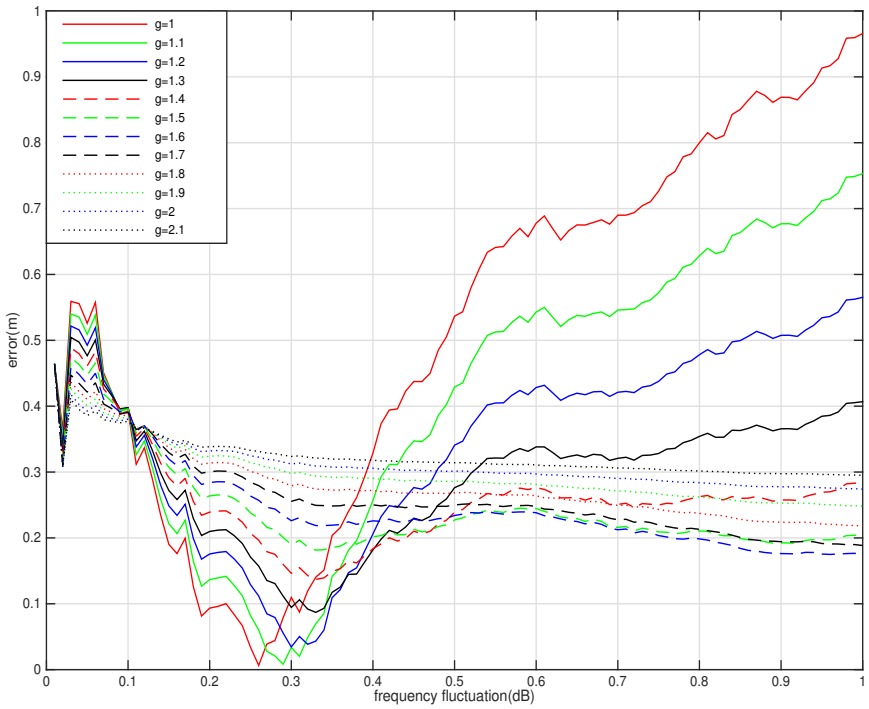

Figure 5.5: Localization error versus path loss fluctuation with different weight function while g is from 1 to 2.1.

fluctuation range is large or put the degree to 1 otherwise.

5.3 Software Defined Radio Platform

We obtain the path loss from the transmitter to the receiver on the SDR platform while changing the carrier frequency. SDR is a radio communication system, but instead of implementing components in hardware typically, it is implemented on a personal computer or embedded system by means of software. SDR implements some or all of the operating functions through modifiable software or firmware on programmable processing technologies. These devices include Field Programmable Gate Arrays (FPGAs), digital signal processors, general purpose processors, programmable System on Chip (SoC) or other application specific programmable processors. SDR technology brings flexibility, cost efficiency, it allows new wireless features and capabilities to be added to existing radio systems without requiring new hardware.

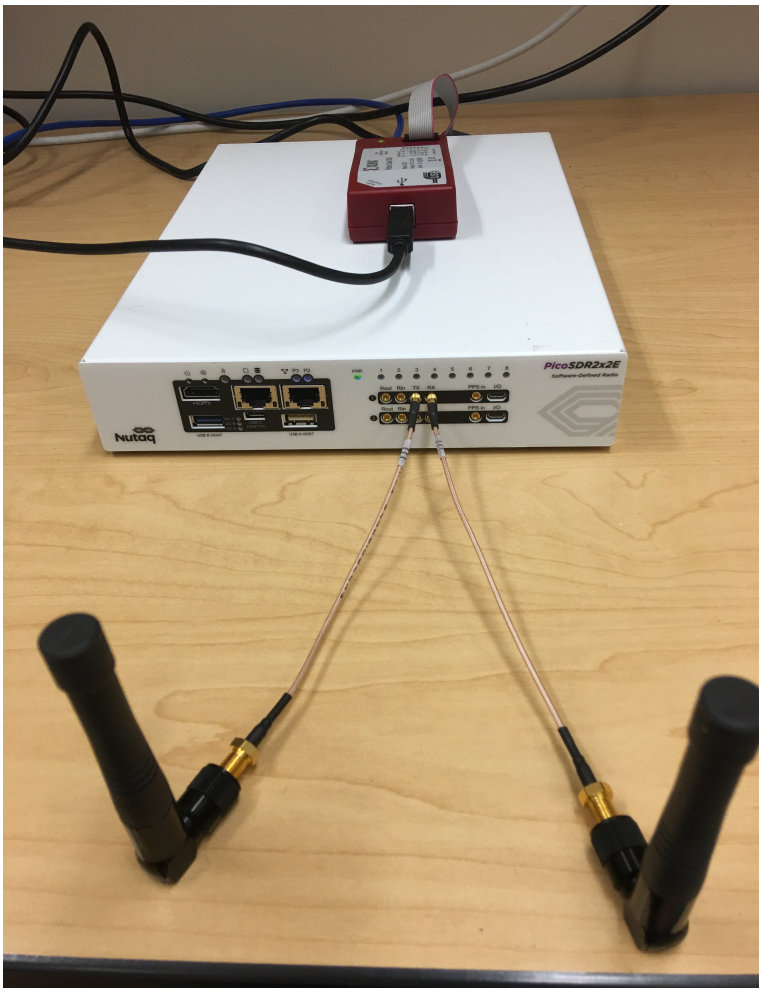

Figure 5.6: SDR platform.

PicoSDR is a table top SDR solution provided by Nutaq which is shown in Figure 5.6 and its radio section which is based on the Nutaq Radio420x FPGA Mezzanine Card (FMC). Its multi-band Radio Frequency (RF) transceivers support operation anywhere between 0.3 GHz and 3.8GHz, frequency division duplex and time division duplex which can be implemented in our multi-frequency localization scheme.

5.3.1 Gain control

Inside the SDR, there are various components having the capability to adjust the gain including the automatic gain control which must be figured out before the experiment. Generally,

the Radio420 FMC embedded in the PicoSDR can be considered as a module which is designed around a multi-band transceiver LMS6002D with a analog RF path on top of the integrated LMS6002D's Variable Gain Amplifiers (VGA) which gives the transmit gain and receive gain between -13.5dB to 18dB.Gain control divides into two parts: transmit(TX) gain and receive(RX) gain.

Transmit gain

Transmit gain is divided into three parts: TX VGA1 gain, TX VGA2 gain and TX gain 3. TX VGA1 gain is a transmit amplifier which can be set from -35dB to -4dB. TX VGA2 gain is a transmit amplifier which can be set from 0 to 25dB. TX gain 3 is a transmit amplifier which can be set from -13 dB to 18dB. TX gain 3 can be controlled by both CLI command and yellow box under Simulink.

Receive gain

The receive gain is divided into four parts: RX LNA gain, RX VGA1 gain, RX gain 2 and RX gain 3. The RX LNA gain can be set to bypass which means 0dB. RX LNA gain can also be set to medium gain and maximum gain by this receive low noise amplifier. RX VGA1 gain can be set to 5dB, 19dB or 30dB where 19dB is the default setting.. RX gain 2 can be set from 0 to 30dB and it has a gain step size of 3dB. RX gain 3 can be set from -13dB to 18dB which can be controlled by both CLI command and yellow box under Simulink.

5.3.2 Implement procedure

We utilize Nutaq's PicoSDR 2×2 to collect the measurements data in different frequencies.

Matlab Simulink diagram: Firstly, we use the blocks provided by Nutaq's Model-Based Design Kit (MBDK) and Simulink to design the system diagram. Then we test and simulate the design to generate the bitstream file which contains configuration information in binary format as well as CDC file for later use in the Microscope. The PicoSDR's FPGAs receive data from the Analog to Digital Converters (ADCs) and send data to the Digital to Analog Converter (DAC) which are demonstrated as the green blocks as shown in Figure 5.7 below.

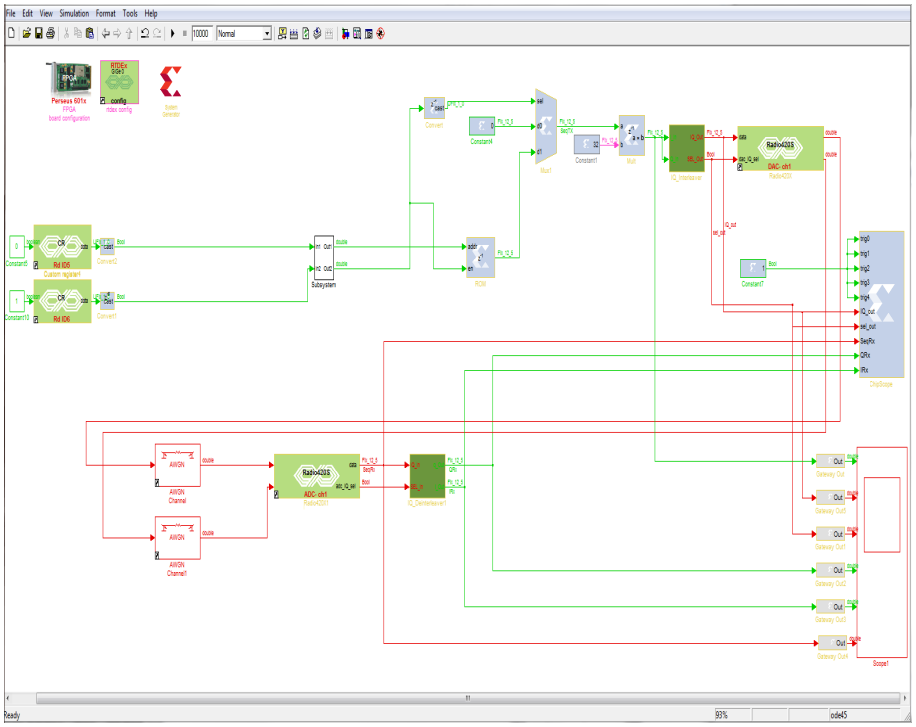

Figure 5.7: Diagram of designed system blocks in Simulink.

iMPACT: Xilinx provides iMPACT to initialize the JTAG (Joint Test Action Group) chain as well as to program the devices. After powering up the SDR and attaching SDR JTAG cable to the parallel port, iMPACT detects the FPGA chips in the SDR by right-clicking on the empty space in the iMPACT window to select "Initialize Chain". After initializing the chain and the devices, we assign the generated Bitstream file (*.bit) to program the device. In this project, since we use PicoSDR 2×2 which is based on a Virtex-6 xc6vsx315t FPGA, we program our generated Bitstream on it as shown in Figure 5.8. When operation is done successfully, the iMPACT window shows the "Programming Succeeded" sign.

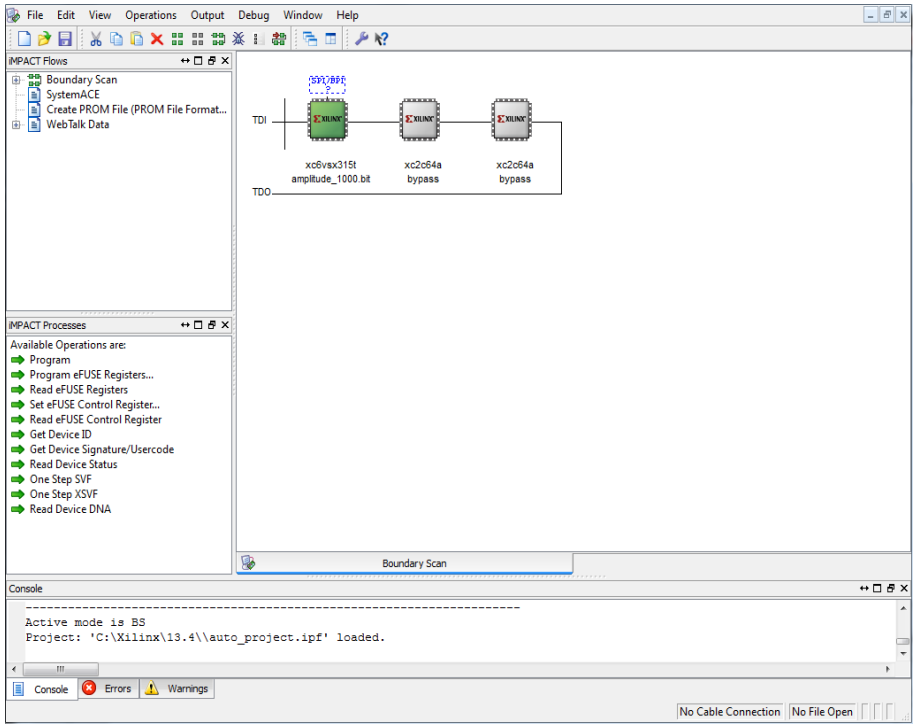

Figure 5.8: Interface of iMPACT software.

Chipscope analyzer: In order to debug our design and observe the input/output data, we make use of the ChipScope block provided by the Xilinx System Generator library. As a result of it, the CDC file is automatically created by the system generator. Open the ChipScope analyzer tool from Xilinx software suite and click the chain square to connect to the platform's FPGA JTAG chain. After importing the CDC file in ChipScope, we can see the waveforms we select by triggering the signal as shown in Figure 5.9. By changing the signal to Signed Decimal, we get the signal amplitudes information.

Command line interface: The Board Software Development Kit (BSDK) provided by Nutaq Perseus-based system contains a feature called the Command Line Interface (CLI). It allows easy access to control the Perseus advanced mezzanine card through application programming interface. We mainly use this feature to control the gain of the transmitter and receiver by sending control commands and streaming data between the host PC and the SDR.

Simulink control: Besides using CLI to control the SDR, Nutaq Co-Simulation tools also pro-

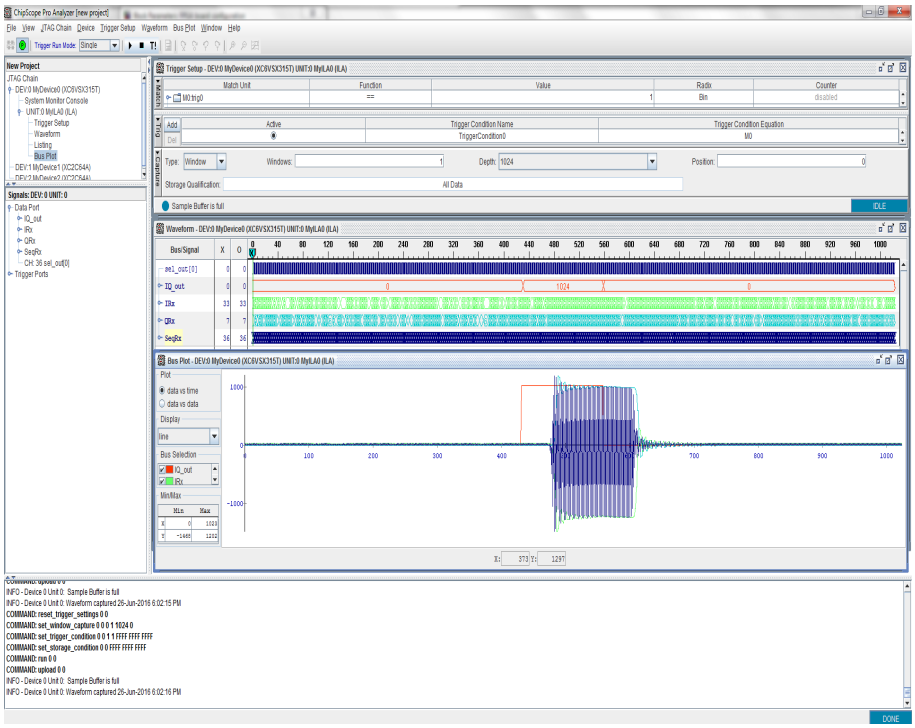

Figure 5.9: Waveforms of selected signals in ChipScope interface.

vides a user defined control register blocksets. The yellow blocks illustrated in Figure 5.10 are kept in the Simulink environment. They hold the System Generator block set implementation of the control algorithm and enable the sending and receiving of data to the system in real time over Gigabit Ethernet.

5.4 Experimental Results

To set up the scenario, we put three transmitters 3 meters away from the target which have the ability to measure the signal strength under different frequencies in a LoS environment. The frequency is a prior knowledge to us instead of having the distance information between the transmitters and receive, we get the localization results not only including the distance information d_1, d_2, d_3 from three transmitters separately but also the path loss exponent n as indicated in Table 5.1.

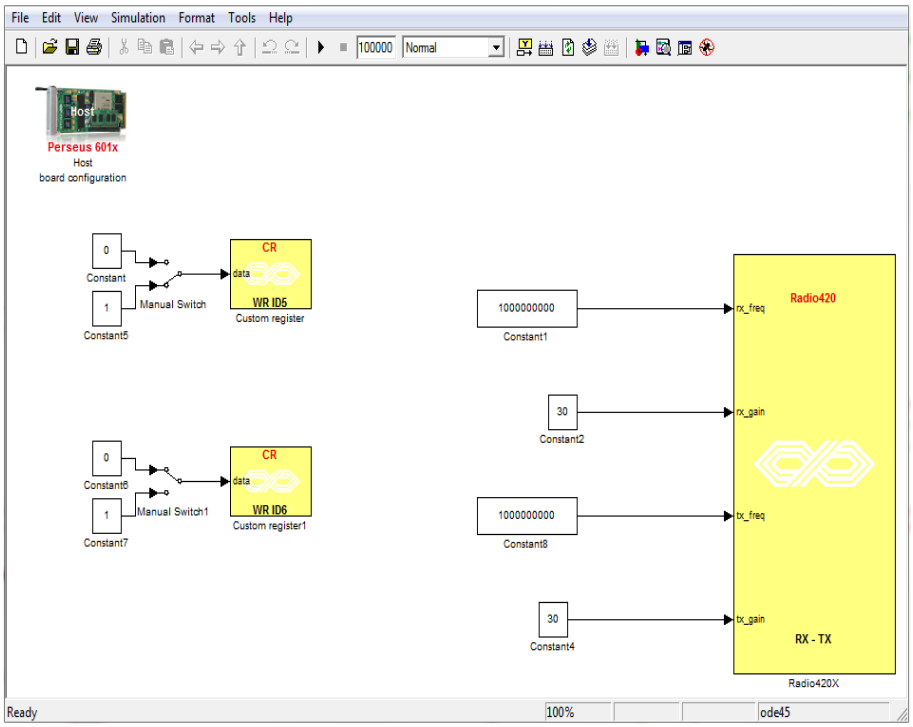

Figure 5.10: Diagram of control blocks in Simulink.

We utilize SDR to imitate WiFi environment which is based on IEEE 802.11 standard and mostly deployed for WLAN applications. As shown in Figure 5.11, with the frequency resolution increasing, the error increases as well. It suggests we can measure multiple different

Frequency(GHz)	Path Loss Exponent n	Distance d_1(m)	Distance d_2(m)	Distance d_3(m)
2.412	3.3312	3.0007	2.6429	3.4069
2.417	3.6728	3	2.96	3.0406
2.422	4.3805	3.0001	2.8023	3.2117
2.427	2.1986	3	3.1961	2.816
2.432	2.2446	3.0002	2.7374	3.2882
2.437	3.2532	3.0001	2.7863	3.2302
2.442	2.277	3.0004	2.6956	3.3395
2.447	2.2284	3.0022	2.5396	3.5491
2.452	2.6842	3.0042	2.4715	3.6517
2.457	2.8658	3	3.1297	2.8757
2.462	2.0061	3	2.8955	3.1082
2.467	2.1391	1.9277	3.6056	3.7091
2.472	2.8813	3.2682	1.9532	4.3027
2.484	2.5978	3.8284	3.47	1.9598

Table 5.1: Measurements under different frequencies

frequencies within a narrow band to increase the localization accuracy.

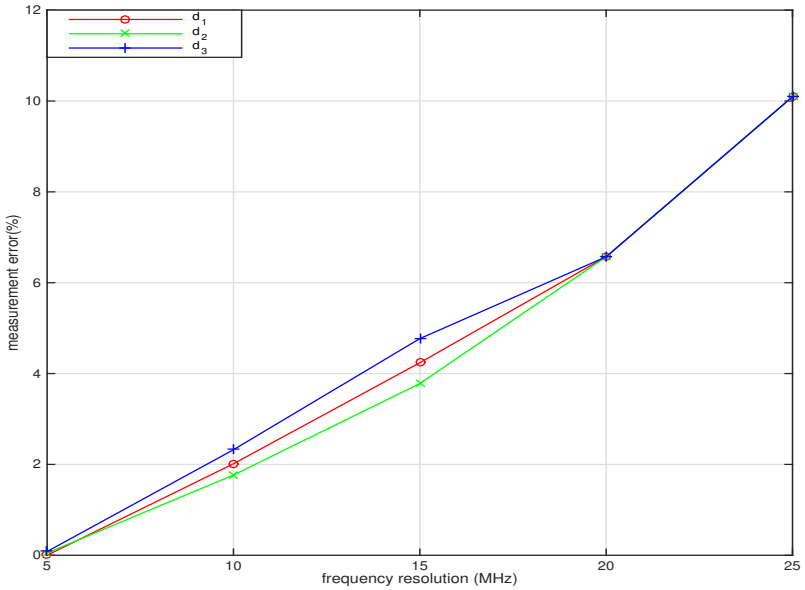

Figure 5.11: Localization error under different frequency resolution.

5.5 Chapter Summary

Instead of having the knowledge of every reference nodes' location and distances to the target, we present how to utilize the carrier frequency information to locate the target. We also present the weighted algorithm to combine path losses under the same frequency but different time in case of the interferences to minimize the localization error. We take experiment on the SDR to collect the real data and it shows lower frequency resolution leads to better performance.

Chapter 6

Conclusion and Future Work

In this thesis, the topic is in the field of localization from three different aspects which are transmitter side, receiver side and signal propagation side. Since reference nodes' location and information are vital and will have large influence on the localization results, the accurate placement of reference nodes is our first research topic. Multiple sensors equipped in smartphone can be utilized for tracking and positioning the user. How to make use of the joint messages is our second topic. Diversed carrier frequencies have impact on RSS measurement which can be used to minimize the positioning error. Proposed algorithms are designed to improve localization accuracy by lowering the average MMSE, combining information from smartphone with RSS measurements and making use of carrier frequency.

The first research topic looks into the MMSE to improves the accuracy of localization. We focus on getting the best placement of RNs as it will greatly influence the performance of position estimation results. An average MMSE within the area of interest has been derived in oder to find the positions of optimum RNs. For further clarifying the algorithm, we present examples in circular, square and hexagonal regions how to place optimum RNs. This scheme can be carried out within any shape of interest and under any measuring technology. For future

possibilities, this reference node placement scheme based on minimizing average error can be further developed to extend the localization range.

Our second proposed algorithm improves the performance by acquiring data from sensors embedded in the smartphone. We also do experiment on iOS platform to show how the acceleration can accumulate as time goes by. Merging accelerometer information with traditional localization technologies can give users insights to tracking them as well as correcting the positioning results. The data from sensors can also be extended to other built-in sensors such as gyroscope and magnetometer in the future.

The third topic is around frequency diversity localization presents how error is being narrowed by utilizing multiple frequencies. Based on the log-distance path loss model in trilateration scenario, instead of providing RNs' locations and path loss exponent information, our scheme only needs frequency information. Weighted scheme based on path loss fluctuation has been presented for better performance. Experiments have been conducted on SDR platform to present path loss on different frequencies. This technique can be combined with power diversity for future research.

Bibliography

[1] Mohapatra, D., & Suma, S. B. (2005, January). Survey of location based wireless services. In *2005 IEEE International Conference on Personal Wireless Communications, 2005. ICPWC 2005.* (pp. 358-362). IEEE.

[2] Carli, M., Panzieri, S., & Pascucci, F. (2014). A joint routing and localization algorithm for emergency scenario. *Ad Hoc Networks, 13*, 19-33.

[3] Chew, S. H., Chong, P. A., Gunawan, E., Goh, K. W., Kim, Y., & Soh, C. B. (2006, August). A hybrid mobile-based patient location tracking system for personal healthcare applications. In *Engineering in Medicine and Biology Society, 2006. EMBS'06. 28th Annual International Conference of the IEEE* (pp. 5188-5191). IEEE.

[4] Stoleru, R., & Stankovic, J. A. (2004, October). Probability grid: A location estimation scheme for wireless sensor networks. In *Sensor and Ad Hoc Communications and Networks, 2004. IEEE SECON 2004. 2004 First Annual IEEE Communications Society Conference on* (pp. 430-438). IEEE.

[5] Simek, M., Moravek, P., Komosny, D., & Dusik, M. (2012). Distributed recognition of reference nodes for wireless sensor network localization. *Radioengineering, 21*(1), 89-98.

[6] Niculescu, D., & Nath, B. (2003). DV based positioning in ad hoc networks. *Telecommunication Systems, 22*(1-4), 267-280.

[7] Han, G., Choi, D., & Lim, W. (2007, October). A novel reference node selection algorithm based on trilateration for indoor sensor networks. In *Computer and Information Technology, 2007. CIT 2007. 7th IEEE International Conference on* (pp. 1003-1008). IEEE.

[8] Noh, A. S. I., Lee, W. J., & Ye, J. Y. (2008, August). Comparison of the mechanisms of the ZigBee's indoor localization algorithm. In *Software Engineering, Artificial Intelligence, Networking, and Parallel/Distributed Computing, 2008. SNPD'08. Ninth ACIS International Conference on* (pp. 13-18). IEEE.

[9] Han, G., Choi, D., & Lim, W. (2009). Reference node placement and selection algorithm based on trilateration for indoor sensor networks. *Wireless Communications and Mobile Computing, 9*(8), 1017-1027.

[10] Azizyan, M., Constandache, I., & Roy Choudhury, R. (2009, September). SurroundSense: mobile phone localization via ambience fingerprinting. In *Proceedings of the 15th annual international conference on Mobile computing and networking* (pp. 261-272). ACM.

[11] Zheng, X., Liu, H., Yang, J., Chen, Y., Martin, R. P., & Li, X. (2014). A study of localization accuracy using multiple frequencies and powers. *IEEE Transactions on Parallel and Distributed Systems, 25*(8), 1955-1965.

[12] Schiller, J., & Voisard, A. (Eds.). (2004). *Location-based services*. Elsevier.

[13] Patwari, N., Ash, J. N., Kyperountas, S., Hero, A. O., Moses, R. L., & Correal, N. S. (2005). Locating the nodes: cooperative localization in wireless sensor networks. *IEEE Signal processing magazine, 22*(4), 54-69.

[14] Franceschini, F., Galetto, M., Maisano, D., & Mastrogiacomo, L. (2009). A review of localization algorithms for distributed wireless sensor networks in manufacturing. *International journal of computer integrated manufacturing, 22*(7), 698-716.

[15] Marcelín-Jiménez, R., Ruiz-Sánchez, M. Á., López-Villaseñor, M., Ramos-Ramos, V. M., Moreno-Escobar, C., & Ruiz-Sandoval, M. E. (2010). A Survey on Localization in Wireless Sensor Networks. *IGI Global*.

[16] Fox, D., Hightower, J., Liao, L., Schulz, D., & Borriello, G. (2003). Bayesian filtering for location estimation. *IEEE pervasive computing, 2*(3), 24-33.

[17] Liu, H., Darabi, H., Banerjee, P., & Liu, J. (2007). Survey of wireless indoor positioning techniques and systems. IEEE Transactions on Systems, Man, and Cybernetics, Part C (Applications and Reviews), 37(6), 1067-1080.

[18] Fontán, F. P., and Espiñeira, P. M. (2008). *Modelling the wireless propagation channel: a simulation approach with Matlab* (Vol. 5). John Wiley & Sons.

[19] Rappaport, T. S. (1996). *Wireless communications: principles and practice* (Vol. 2). New Jersey: Prentice Hall PTR.

[20] Kushki, A., Plataniotis, K. N., & Venetsanopoulos, A. N. (2007). Kernel-based positioning in wireless local area networks. *IEEE transactions on mobile computing, 6*(6), 689-705.

[21] Li, X. (2006). RSS-based location estimation with unknown pathloss model. *IEEE Transactions on Wireless Communications, 5*(12), 3626-3633.

[22] Elnahrawy, E., Li, X., & Martin, R. P. (2004, October). The limits of localization using signal strength: A comparative study. In *Sensor and Ad Hoc Communications and Networks, 2004. IEEE SECON 2004. 2004 First Annual IEEE Communications Society Conference on* (pp. 406-414). IEEE.

[23] Whitehouse, K., Karlof, C., & Culler, D. (2007). A practical evaluation of radio signal strength for ranging-based localization. *ACM SIGMOBILE Mobile Computing and Communications Review, 11*(1), 41-52.

[24] Baala, O., Zheng, Y., & Caminada, A. (2009, March). The impact of AP placement in WLAN-based indoor positioning system. In *2009 Eighth International Conference on Networks.*

[25] Liu, H., Darabi, H., Banerjee, P., & Liu, J. (2007). Survey of wireless indoor positioning techniques and systems. *IEEE Transactions on Systems, Man, and Cybernetics, Part C (Applications and Reviews)*, 37(6), 1067-1080.

[26] Gezici, S., Tian, Z., Giannakis, G. B., Kobayashi, H., Molisch, A. F., Poor, H. V., & Sahinoglu, Z. (2005). Localization via ultra-wideband radios: a look at positioning aspects for future sensor networks. *IEEE signal processing magazine*, 22(4), 70-84.

[27] Römer, K., Blum, P., & Meier, L. (2005). Time synchronization and calibration in wireless sensor networks. *Handbook of Sensor Networks: Algorithms and Architectures, 49*, 199.

[28] Jardak, N., & Samama, N. (2009). Indoor positioning based on GPS-repeaters: performance enhancement using an open code loop architecture. *IEEE Transactions on Aerospace and electronic systems*, 45(1), 347-359.

[29] Rabinowitz, M., & Spilker, J. J. (2005). A new positioning system using television synchronization signals. *IEEE Transactions on Broadcasting*, 51(1), 51-61.

[30] Cheung, K. W., So, H. C., Ma, W. K., & Chan, Y. T. (2006). A constrained least squares approach to mobile positioning: algorithms and optimality. EURASIP Journal on Advances in Signal Processing, 2006(1), 1-23.

[31] Zhou, J., Zhang, H., & Mo, L. (2011, May). Two-dimension localization of passive RFID tags using AOA estimation. In *Instrumentation and Measurement Technology Conference (I2MTC), 2011 IEEE* (pp. 1-5). IEEE.

[32] Leon, S. J. (1980). *Linear algebra with applications* (pp. 283-313). New York: Macmillan.

[33] Stigler, S. M. (1986). *The history of statistics: The measurement of uncertainty before 1900*. Harvard University Press.

[34] Legendre, A. M. (1805). *Nouvelles mthodes pour la dtermination des orbites des comtes* (No. 1). F. Didot.

[35] Pfanzagl, J. (1994). *Parametric statistical theory*. Walter de Gruyter.

[36] Cramr, H. (1947). Mathematical methods of statistics.

[37] Rao, C. R. (1992). Information and the accuracy attainable in the estimation of statistical parameters. In *Breakthroughs in statistics* (pp. 235-247). Springer New York.

[38] Wang, H., Sen, S., Elgohary, A., Farid, M., Youssef, M., & Choudhury, R. R. (2012, June). No need to war-drive: unsupervised indoor localization. In *Proceedings of the 10th international conference on Mobile systems, applications, and services* (pp. 197-210). ACM.

[39] Liu, H. H., & Pang, G. K. (2001). Accelerometer for mobile robot positioning. IEEE Transactions on Industry Applications, 37(3), 812-819.

[40] Pahlavan, K., & Levesque, A. H. (2005). *Wireless information networks* (Vol. 93). John Wiley & Sons.

[41] Klepal, M., & Pesch, D. (2007, March). Influence of predicted and measured fingerprint on the accuracy of RSSI-based indoor location systems. In *2007 4th Workshop on Positioning, Navigation and Communication* (pp. 145-151). IEEE.

[42] Rejane, D., Thierry, V., & Adrien Van Den, B. (2011). Comparison of indoor localization systems based on wireless communications. *Wireless Engineering and Technology, 2011*.

[43] Bahl, P., & Padmanabhan, V. N. (2000). RADAR: An in-building RF-based user location and tracking system. In *INFOCOM 2000. Nineteenth Annual Joint Conference of the IEEE Computer and Communications Societies. Proceedings. IEEE* (Vol. 2, pp. 775-784). Ieee.

[44] Varshavsky, A., De Lara, E., Hightower, J., LaMarca, A., & Otsason, V. (2007). GSM indoor localization. *Pervasive and Mobile Computing, 3*(6), 698-720.

[45] Salman, N., Ghogho, M., & Kemp, A. H. (2014). Optimized low complexity sensor node positioning in wireless sensor networks. *IEEE Sensors Journal, 14*(1), 39-46.

[46] Shen, J., Molisch, A. F., & Salmi, J. (2012). Accurate passive location estimation using TOA measurements. *IEEE Transactions on Wireless Communications, 11*(6), 2182-2192.

[47] Qi, Y., Kobayashi, H., & Suda, H. (2006). Analysis of wireless geolocation in a non-line-of-sight environment. *IEEE Transactions on wireless communications, 5*(3), 672-681.

[48] Gezici, S. (2008). A survey on wireless position estimation. *Wireless personal communications, 44*(3), 263-282.

[49] Monica, S., & Ferrari, G. (2015). UWB-based localization in large indoor scenarios: Optimized placement of anchor nodes. *IEEE Transactions on Aerospace and Electronic Systems, 51*(2), 987-999.

[50] Rao, C. R. (2009). *Linear statistical inference and its applications* (Vol. 22). John Wiley & Sons.

[51] Liu, Y., Yang, Z., Wang, X., & Jian, L. (2010). Location, localization, and localizability. *Journal of Computer Science and Technology, 25(2),* 274-297.

[52] Lin, C.-C., Chiu, M.-J., Hsiao, C.-C., Lee, R.-G., & Tsai, Y.-S. (2006). Wireless health care service system for elderly with dementia. *Information Technology in Biomedicine, IEEE Transactions on, 10*(4), 696-704.

[53] Wu, C. L., & Fu, L. C. (2012). Design and realization of a framework for humansystem interaction in smart homes. *Systems, Man and Cybernetics, Part A: Systems and Humans, IEEE Transactions on, 42*(1), 15-31.

[54] Xiuquan, Q., Jianchong, S., Jinsong, Z., Wangli, X., Budan, W., Sida, X., & Junliang, C. (2014). Recommending friends instantly in location-based mobile social networks. *Communications, China, 11*(2), 109-127.

[55] Stingl, D., Gross, C., Nobach, L., Steinmetz, R., & Hausheer, D. (2013, October). Block-Tree: Location-aware decentralized monitoring in mobile ad hoc networks. In *Local Computer Networks (LCN), 2013 IEEE 38th Conference on* (pp. 373-381). IEEE.

[56] Walter, O., Schmalenstroeer, J., Engler, A., & Haeb-Umbach, R. (2013, March). Smartphone-based sensor fusion for improved vehicular navigation. In *Positioning Navigation and Communication (WPNC), 2013 10th Workshop on* (pp. 1-6). IEEE.

[57] Spirito, M. A. (2001). On the accuracy of cellular mobile station location estimation. *Vehicular Technology, IEEE Transactions on, 50*(3), 674-685.

[58] Lv, X., Mourad-Chehade, F., & Snoussi, H. (2013, December). Fingerprinting-based localization using accelerometer information in wireless sensor networks. In *Global Communications Conference (GLOBECOM), 2013 IEEE* (pp. 510-515). IEEE.

[59] Sharp, I., & Yu, K. (2014). Indoor TOA error measurement, modeling, and analysis. *Instrumentation and Measurement, IEEE Transactions on, 63*(9), 2129-2144.

[60] Shao, H. J., Zhang, X. P., & Wang, Z. (2014). Efficient closed-form algorithms for AOA based self-localization of sensor nodes using auxiliary variables. *Signal Processing, IEEE Transactions on, 62*(10), 2580-2594.

[61] Tong, K., Wang, X., Khabbazibasmenj, A., & Dounavis, A. (2014, September). RSS-Based Localization in Obstructed Environment with Unknown Path Loss Exponent. In *Vehicular Technology Conference (VTC Fall), 2014 IEEE 80th* (pp. 1-5). IEEE.

[62] Subbu, K., Zhang, C., Luo, J., & Vasilakos, A. (2014). Analysis and status quo of smartphone-based indoor localization systems. *Wireless Communications, IEEE, 21*(4), 106-112.

[63] Torres-Solis, J., Falk, T. H., & Chau, T. (2010). *A review of indoor localization technologies: towards navigational assistance for topographical disorientation.* INTECH Open Access Publisher.

[64] Deng, B., Huang, G., Zhang, L., & Liu, H. (2008, November). Improved centroid localization algorithm in WSNs. In *Intelligent System and Knowledge Engineering, 2008. ISKE 2008. 3rd International Conference on* (Vol. 1, pp. 1260-1264). IEEE.

[65] Bulusu, N., Heidemann, J., & Estrin, D. (2000). GPS-less low-cost outdoor localization for very small devices. *IEEE personal communications, 7*(5), 28-34.

[66] Blumenthal, J., Grossmann, R., Golatowski, F., & Timmermann, D. (2007, October). Weighted centroid localization in zigbee-based sensor networks. In *Intelligent Signal Processing, 2007. WISP 2007. IEEE International Symposium on* (pp. 1-6). IEEE.

[67] Fink, A., & Beikirch, H. (2009, March). RSSI-based indoor localization using antenna diversity and plausibility filter. In *Positioning, Navigation and Communication, 2009. WPNC 2009. 6th Workshop on* (pp. 159-165). IEEE.

[68] Fink, A., Beikirch, H., Voß, M., & Schröder, C. (2010, September). RSSI-based indoor positioning using diversity and Inertial Navigation. In *Indoor Positioning and Indoor Navigation (IPIN), 2010 International Conference on* (pp. 1-7). IEEE.

[69] Garg, V. (2010). *Wireless communications & networking*. Morgan Kaufmann.

[70] Savvides, A., Park, H., & Srivastava, M. B. (2002, September). The bits and flops of the n-hop multilateration primitive for node localization problems. In *Proceedings of the 1st ACM international workshop on Wireless sensor networks and applications* (pp. 112-121). ACM.

[71] Moore, D., Leonard, J., Rus, D., & Teller, S. (2004, November). Robust distributed network localization with noisy range measurements. In *Proceedings of the 2nd international conference on Embedded networked sensor systems* (pp. 50-61). ACM.

[72] Yang, Z., & Liu, Y. (2010). Quality of trilateration: Confidence-based iterative localization. *IEEE Transactions on Parallel and Distributed Systems, 21*(5), 631-640.

Curriculum Vitae

Name:	Fei Long
Post-Secondary Education and Degrees:	2014 - present, M.E.Sc Electrical and Computer Engineering University of Western Ontario London, Ontario, Canada 2010 - 2014, B.Eng University of Electronic Science and Technology of China Chengdu, Sichuan, China
Honours and Awards:	NSERC CREATE Scholar 2014-2016
Related Work Experience:	Teaching Assistant The University of Western Ontario 2014 - 2016

Publications:

[1] Long, F., Behnad, A., & Wang, X. (2015, December). Optimum reference node deployment for indoor localization based on the average Mean Square Error minimization. In *2015 IEEE 34th International Performance Computing and Communications Conference (IPCCC)* (pp. 1-6). IEEE.

[2] Long, F., Tong, K., & Wang, X. (2016, November). Joint localization algorithm combining information from accelerometer and available reference nodes. In *Information Technology,*

Electronics and Mobile Communication Conference (IEMCON), 2016 IEEE 7th Annual (pp. 1-6). IEEE.